Int J Earth Sci (Geol Rundsch) (2006) 95: 609–627
DOI 10.1007/s00531-005-0058-2

ORIGINAL PAPER

Osman Parlak

Geodynamic significance of granitoid magmatism in the southeast Anatolian orogen: geochemical and geochronogical evidence from Göksun–Afşin (Kahramanmaraş, Turkey) region

Received: 27 August 2004 / Accepted: 22 October 2005 / Published online: 7 December 2005

Abstract In southeast Anatolia, there are number of tectonomagmatic units in the Kahramanmaraş–Malatya–Elazığ region that are important in understanding the geological evolution of the southeast Anatolian orogenic belt during the Late Cretaceous. These are (a) metamorphic massifs, (b) ophiolites, (c) ophiolite-related metamorphics and (d) granitoids. The granitoids (i.e. Göksun–Afşin in Kahramanmaraş, Doğanşehir in Malatya and Baskil in Elazığ) intrude all the former units in a NE–SW trending direction. The granitoid in Göksun–Afşin (Kahramanmaraş) region is mainly composed of granodioritic and granitic in composition. The granodiorite contains a number of amphibole-bearing mafic microgranular enclaves of different sizes, whereas the granite is intruded by numerous aplitic dikes. The granitoid rocks have typical calcalkaline geochemical features. The REE- and Ocean ridge granite-normalized multi-element patterns and tectonomagmatic discrimination diagrams, as well as biotite geochemistry suggest that the granitoids were formed in a volcanic arc setting. The K–Ar geochronology of the granitoid rocks yielded ages ranging from 85.76 ± 3.17 to 77.49 ± 1.91 Ma. The field, geochemical and geochronological data suggest the following Late Cretaceous tectonomagmatic scenario for southeast Anatolia. The ophiolites were formed in a suprasubduction zone tectonic setting whereas the ophiolite-related metamorphic rocks formed either during the initiation of intraoceanic subduction or late-thrusting (~90 Ma). These units were then overthrust by the Malatya–Keban platform during the progressive elimination of the southern Neotethys. Thrusting of the Malatya–Keban platform over the ophiolites and related metamorphic rocks was followed by the intrusion of the granitoids (88–85 Ma) along the Tauride active continental margin in the southern Neotethys.

O. Parlak (✉)
Mühendislik-Mimarlık Fakültesi, Jeoloji Mühendisliği Bölümü,
Çukurova Üniversitesi, 01330 Balcalı, Adana, Turkey
E-mail: parlak@cukurova.edu.tr
Tel.: +90-322-3387081
Fax: +90-322-3386715

Keywords Southeast Anatolia · Volcanic arc · Granitoids · Active margin · Late Cretaceous

Introduction

Turkey occupies a critical segment in the Alpine–Himalayan orogenic system, where remnants of both the Paleotethyan and Neotethyan ocean basins crop out between nearly E–W trending tectonic belts, such as the Pontides, Anatolides, Taurides and the Border folds (Ketin 1983) (Fig. 1a). Most of the evidence related to the Paleotethyan evolution lies in the Sakarya zone (Karakaya complex) and Central Pontides in the north and northwestern Turkey and is characterized by a tectonic collage of various units covered unconformably by Liassic sediments (Şengör and Yılmaz 1981; Pickett and Robertson 1996), whereas the Neotethyan event was active throughout the Anatolia between the Triassic and the Miocene (Şengör and Yılmaz 1981; Robertson and Dixon 1984). The Neotethyan subduction zones are traced by the E–W trending belts of Late Cretaceous ophiolites and related rocks obducted onto the platform carbonates during the closure of the oceanic basins in between the metamorphic massifs of the Anatolia.

Mesozoic- to Cenozoic-aged granitoids related to closure of the Neotethys are extensively observed as intruding the metamorphic massifs, platform units, ophiolites and post-Mesozoic (Early Tertiary) rocks throughout Turkey. The granitoids in the southeast Anatolian orogeny are Late Cretaceous in age. The granitoids are wide spread in Kahramanmaraş, Malatya and Elazığ regions (Fig. 2) and are intrusive into the metamorphic platform carbonates (i.e. Malatya, Keban), ophiolites (Göksun, Berit, İspendere and Kömürhan) and volcanic arc units (Yüksekova/Elazığ magmatics) of the southeast Anatolia (Tarhan 1986; Yazgan and Chessex 1991; Yılmaz et al. 1993; Parlak and Rızaoğlu 2004; Robertson et al. 2006a). The only available K–Ar isotopic age determinations range from 76 ± 2.45 and 78 ± 2.5 Ma from the Baskil (Elazığ) area

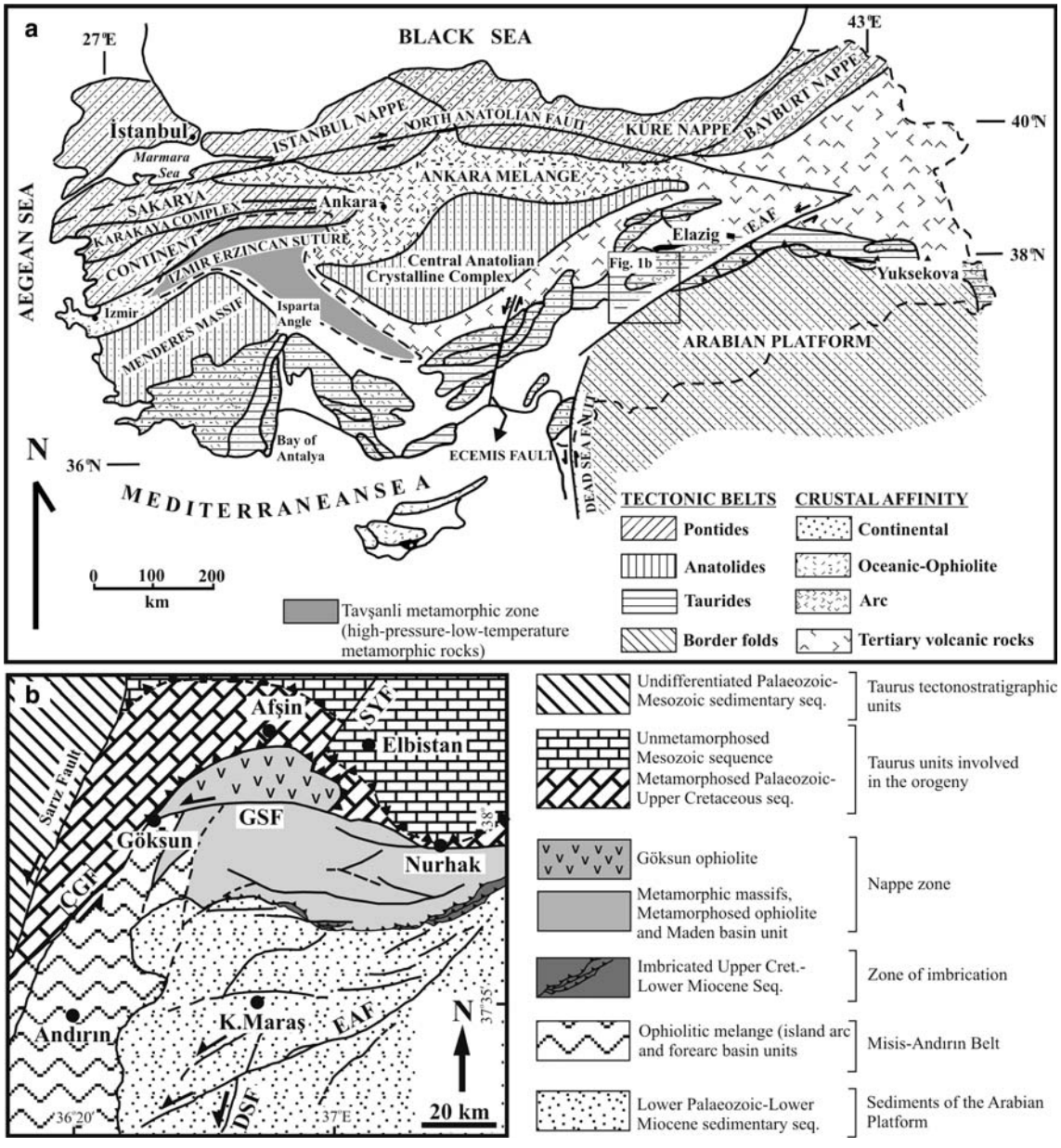

Fig. 1 **a** Major tectonic belts and suture zones of Turkey (from Dilek et al. 1999). **b** Tectonic units and structural features of the Kahramanmaraş–Elbistan regions (Simplified from Yılmaz 1993). Key to the abbreviations: *EAF* East Anatolian Fault, *DSF* Dead Sea Fault, *ÇGF* Çiçekli-Göksun Fault, *GSF* Göksun-Sürgü Fault, *SYF* Sarıyatak Fault

(Yazgan and Chessex 1991). No detailed geochemical analyses have been published for the granitoids in the region so far. Therefore, the geodynamic significance of the felsic intrusions is not well constrained. This paper presents new geochemical and K–Ar geochronological data on the granitoid rocks of the Göksun–Afşin (Kahramanmaraş) region (1) to describe compositional features, (2) to determine their tectonic setting and (3) to show their importance within the Late Cretaceous collisional setting of Neotethys between the Tauride platform and ensimatic island arc units of the Southeast Anatolian Orogen.

Regional geology

Southeast Anatolian orogen comprises three distinct, approximately E–W trending, tectonic units which are separated from one another by major north-dipping thrust faults (Fig. 1b). From north to south these are the nappe zone, the zone of imbrication and the Arabian platform (Yılmaz 1990, 1993; Yılmaz et al. 1993). The nappe zone forms, morphologically, the highest tectonic unit which consists of two large nappes, the Lower and the Upper nappes (Yılmaz 1993). The Lower nappe is

mainly characterized by the variably metamorphosed ophiolitic units and the Maden Group whereas the Upper nappe is represented by the metamorphic massifs (Bitlis, Pütürge, Malatya, Keban, Engizek and Binboğa) of southeast Anatolia (Ketin 1983; Yılmaz 1993). The imbrication zone is a narrow E–W trending belt which was squeezed between the nappe region to the north and the Arabian platform to the south (Fig. 1b). The zone of imbrication is represented by a number of north dipping thrust slices with southerly vergence (Yılmaz et al. 1987; Yılmaz 1990; Karig and Kozlu 1990). The rock units in the imbricated thrust sheets range in age from Late Cretaceous to Early Miocene (Yılmaz 1993). Further to the west-southwest, the rock units of the imbrication zone are traced along the Misis–Andırın Mountain belt (Yılmaz et al. 1987; Yılmaz 1990; Kelling et al. 1987; Robertson et al. 2004, 2006a). The Arabian platform comprises autochthonous and parautochthonous sedimentary units deposited since Early Paleozoic time (Fig. 1b), the tectonically emplaced Upper Cretaceous ophiolites and their sedimentary cover (Yılmaz 1993).

The granitoids related to the subduction of the southern Neotethyan oceanic crust in the southeast Anatolia are observed at three localities namely the Göksun–Afşin (Kahramanmaraş), Doğanşehir (Malatya) and Baskil (Elazığ) regions (Fig. 2). They intrude the tectonostratigraphic and magmatic units of the nappe zone (Yılmaz 1993). The most important point at these localities is that the granitoids are seen as intruding the Malatya–Keban platform, ophiolites and ophiolite-related metamorphics, suggesting that the Malatya–Keban platform and ophiolitic units had been tectonically juxtaposed before the intrusions took place in Late Cretaceous (Yazgan and Chessex 1991; Michard et al. 1984; Perinçek and Kozlu 1984; Robertson et al. 2004). The Göksun–Afşin (Kahramanmaraş) region comprises the Malatya–Keban platform, Göksun ophiolite, granitoid rocks and post-Mesozoic sedimentary units (Fig. 3). The Malatya metamorphics crop out at different localities of the study area as distrupted and fragmented above the ophiolitic units (Fig. 3). The Malatya metamorphics in the Göksun–Afşin region is represented by dark-grey limestone, calcschist, marble, crystallized limestone, phyllite and the occasional pelitic schists. The carbonate rocks at the top of the Malatya metamorphics have yielded an Upper Permian age (Perinçek and Kozlu 1984). However, Yılmaz et al. (1993) stated that the metamorphic massifs of the southeast Anatolia are similar to each other in terms lithology, stratigraphy and structural features and that they yield an age ranging from Permian to Campanian. The Late Cretaceous Göksun ophiolite, tectonically underlying the Malatya metamorphics, is represented by a complete oceanic crustal section between Göksun and Afşin (Kahramanmaraş) region (Fig. 3). From bottom to top, it comprises serpentinized mantle tectonites, ultramafic to mafic cumulates, isotropic gabbro, sheeted dikes and extrusives represented by wide variety of volcanic rocks from basalt to rhyolite (Fig. 4) (Perinçek and Kozlu 1984; Yılmaz 1993; Yılmaz et al. 1993; Parlak et al. 2004). The granitoid body forms two SW–NE trending bands in the west, merging into a single unit, up to 4 km, across in the east along the Göksun river (Perincek and Kozlu 1984; Robertson et al. 2006a). It crops out at Göksun, Karaömer, Deveboynu and Kargabükü (Fig. 3). It has intrusive contact relations with the ophiolitic units and is overlain by the Cenozoic cover sediments (Fig. 3). Although intrusive contact relationship between the granitoid and the Malatya–Keban platform is obscured in the Göksun (Kahramanmaraş) area, it is well constrained in Doğanşehir (Malatya) and Baskil (Elazığ) regions in the east of present study area (Fig. 2). The rock types in the granitoid are mainly granodioritic and

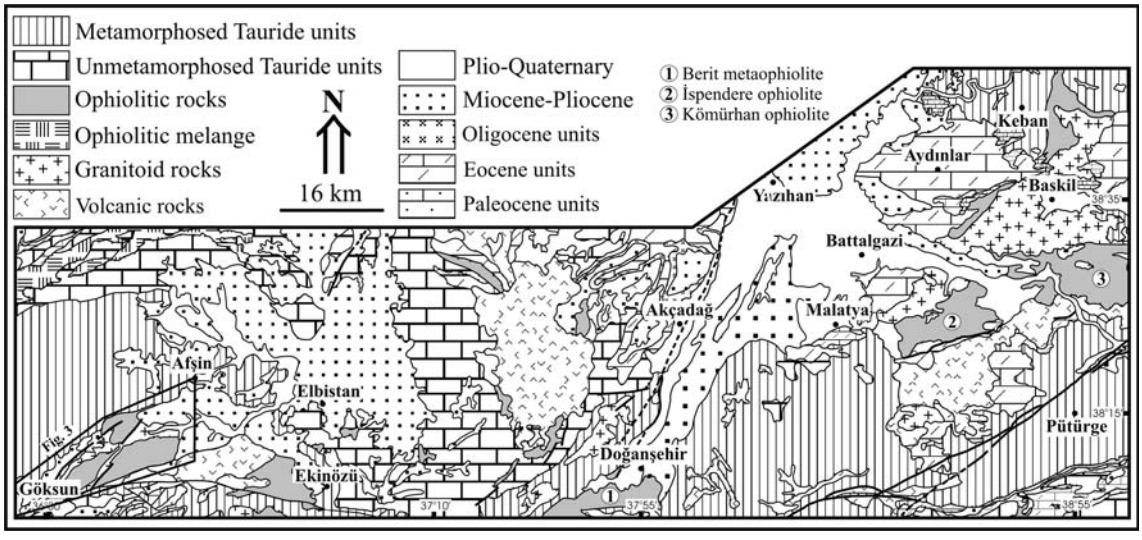

Fig. 2 Simplified geological map of the area between Göksun (Kahramanmaraş) and Baskil (Elazığ), showing the distribution of Late Cretaceous granitoids (simplified from MTA 2002). Location of Fig. 3 is also shown

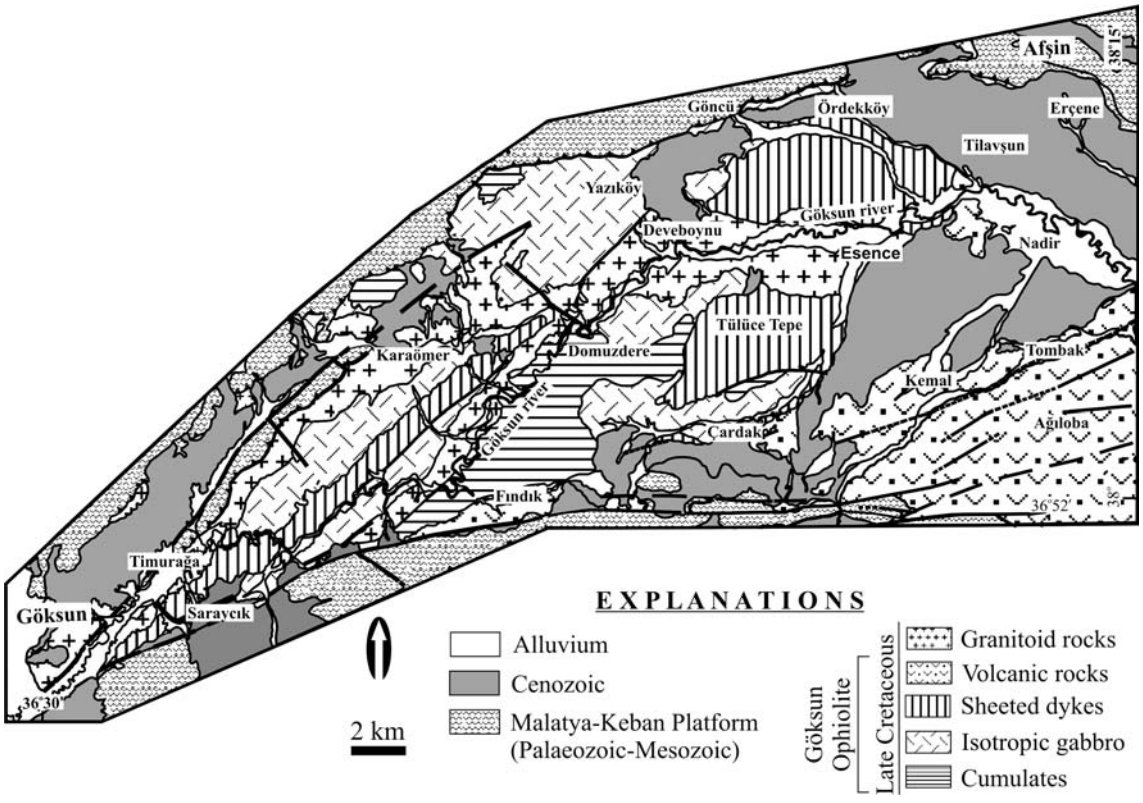

Fig. 3 Geological map of the Göksun–Afşin (Kahramanmaraş) region (modified from Perinçek and Kozlu 1984)

granitic in composition. The granodiorites are relatively fresh at outcrop scale whereas the granites are more altered and show extensive arenitization. The granodiorites contain a number of ellipsoidal mafic microgranular enclaves (MME) of different sizes (Fig. 6a), especially in the north of Tülüce Tepe (Fig. 3). The granites are commonly intruded by aplitic dikes as seen between Deveboynu and Domuzdere (Fig. 3).

Analytical methods

A total of 46 samples from the granitoid rocks were analysed for major and trace elements by XRF in the Mineralogy Department at the University of Geneva. The major element contents were determined on glass beads fused from ignited powders to which $Li_2B_4O_7$ was added at a ratio 1:5, in a gold–platinum crucible at 1,150°C. The trace element contents were measured by XRF on pressed-powder pellets. A subset of representative eight samples were analysed by ICP-MS for trace elements (including REE) at Actlabs-Activation Laboratories in Canada. Four representative polished sections from granodiorites were used for electron microprobe analysis on a JEOL JXA-8600 in the Geology and Paleontology Department at Salzburg University (Austria). The analytical conditions for the elements were 13 s (10 s for Peak and 3 s for Background) of counting interval, beam current −20 nA and acceleration voltage −15 kV. Thirteen biotite and one hornblende separates from the granodiorites were selected for K–Ar analysis in the geochronology laboratory of the Mineralogy Department at Geneva University (Switzerland) in order to determine their relation within the regional geological context. The K content of each sample was measured by Atomic Absortion Spectrometers (AAS). Ar was extracted by total sample fusion into a pyrex line fitted with high vacuum metal valves. The resultant gas was mixed with a ^{38}Ar spike to apply the isotopic dilution technique. The contamining gasses were separated with titanium traps and liquid nitrogen. Measurements were done in static mode with an AEI MS-10S spectrometer fitted with a permanent magnet of 4.1 kG. Samples were degassed at about 100°C for several hours before the analysis to reduce atmospheric contamination. Analytical precision is near 0.5%. To calculate the age, Steiger and Jager (1977) constants were used. The results of geochemical and geochronological analyses are presented in Table. 1, 2, 3, 4, 5, 6.

Petrography and mineralogy

The granitoid rocks in the Göksun–Afşin region are represented by two main groups. The first group is dominated by medium to coarse-grained granodiorites and also transitional between granite and quartz

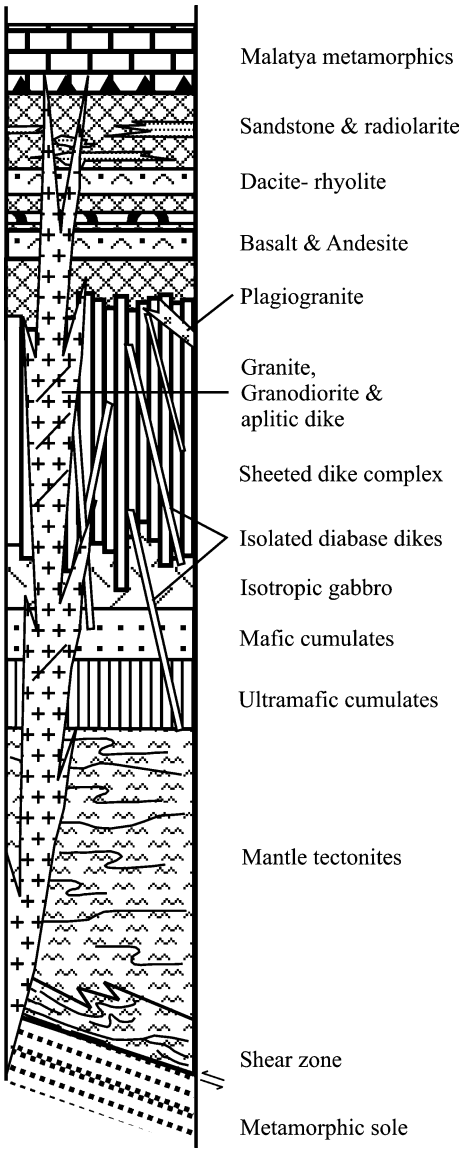

Fig. 4 Synthetic log, showing the relations of the ophiolites, the metamorphic soles, the Tauride platform and the granitoid rocks in southeast Anatolia

monzodiorite (Fig. 5). These rocks contain amphibole-bearing MME in different sizes ranging from 5 to 30 cm (Fig. 6a). They present a granular texture and are composed of quartz (15–30 vol. %), plagioclase (44–62 vol. %), K-feldspar (17–32 vol. %), hornblende (3–5 vol. %) and biotite (3–5 vol. %) (Fig. 6c, d). The accessory phases are titanite and iron-oxides. The granodiorite displays variable degrees of low-temperature alteration minerals, including kaolinite, sericite, calcite and chlorite. The MME in granodiorites are dioritic in composition. They present microgranular texture and are mainly composed of plagioclase (50%), hornblende (35%), K-feldspar (7–8%), quartz (1–2%) and iron oxide minerals. The second group is represented by granites and exhibits granular and micrographic textures. They are composed of quartz (35–42 vol. %), plagioclase (25–38 vol. %), K-feldspar (22–38 vol. %), biotite (3–4 vol. %) and hornblende (1–2 vol. %) (Fig. 6e). They contain low-temperature alteration minerals such as sericite, kaolinite, chlorite, epidote and prehnite. The aplitic dykes present micrographic texture and are composed of quartz (34–43 vol. %), orthoclase (27–35 vol. %), plagioclase (28–47 vol. %), biotite (1–2 vol. %), muscovite (1–2 vol. %) and iron-oxide minerals (Fig. 6b, f).

Mineral chemistry analysis was only performed on granodiorite samples because the granitic rocks have suffered low-temperature alteration. Therefore, four samples of the granodiorites were chosen to characterize the compositions of felsic and mafic mineral phases. The plagioclases are present as subhedral to anhedral crystals in granodiorites. They exhibit both normal ($An_{60–30}$) and reverse ($An_{42–46}$) zoning (Table 1) (Fig. 6c). The plagioclases have a wide range of compositions from labradorite (An_{66}) to oligoclase (An_{11}) (Fig. 7a). The K-feldspars in granodiorites are present as subhedral and anhedral crystals, and exhibit perthitic texture and carlsbad twining. They are dominated by an orthoclase component ($Or_{96–81}$, $Ab_{18–3}$, $An_{0.5–0}$) (Fig. 7a) (Table 1). The Fig. 7a shows the isotherms of temperatures for feldspars based on the experimental study of Fuhrman and Lindsley (1988). The analysed samples plot below the isotherms of 700°C, suggesting that the feldspars of the granodiorites crystallized around 650 ± 50°C (Fig. 7a).

The hornblendes in granodiorites are exclusively represented by magnesiohornblende based on the classification of Leake et al. (1997) (Fig. 7b) (Table 2). The Mg# ($Mg/Mg + Fe^{+2}$) ranges from 0.8 to 0.64 (Table 2). Some of the hornblendes analyses show zoning, as indicated by high Mg (3.03) content in the cores and

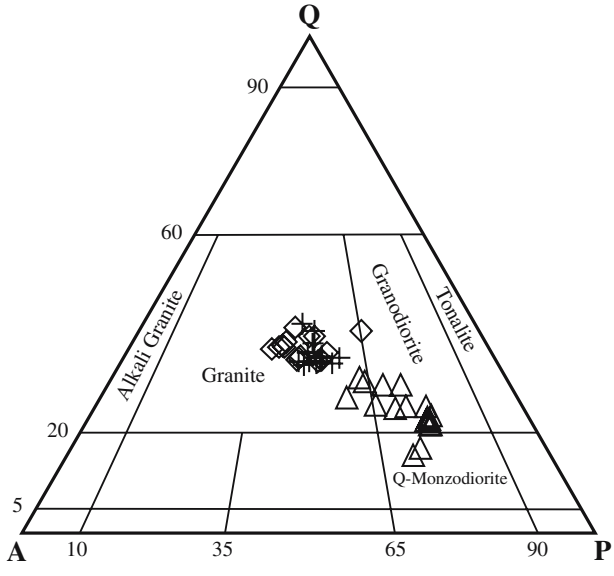

Fig. 5 QAP nomenclature diagram of the granitoid rocks (adapted from Le Maitre 1989)

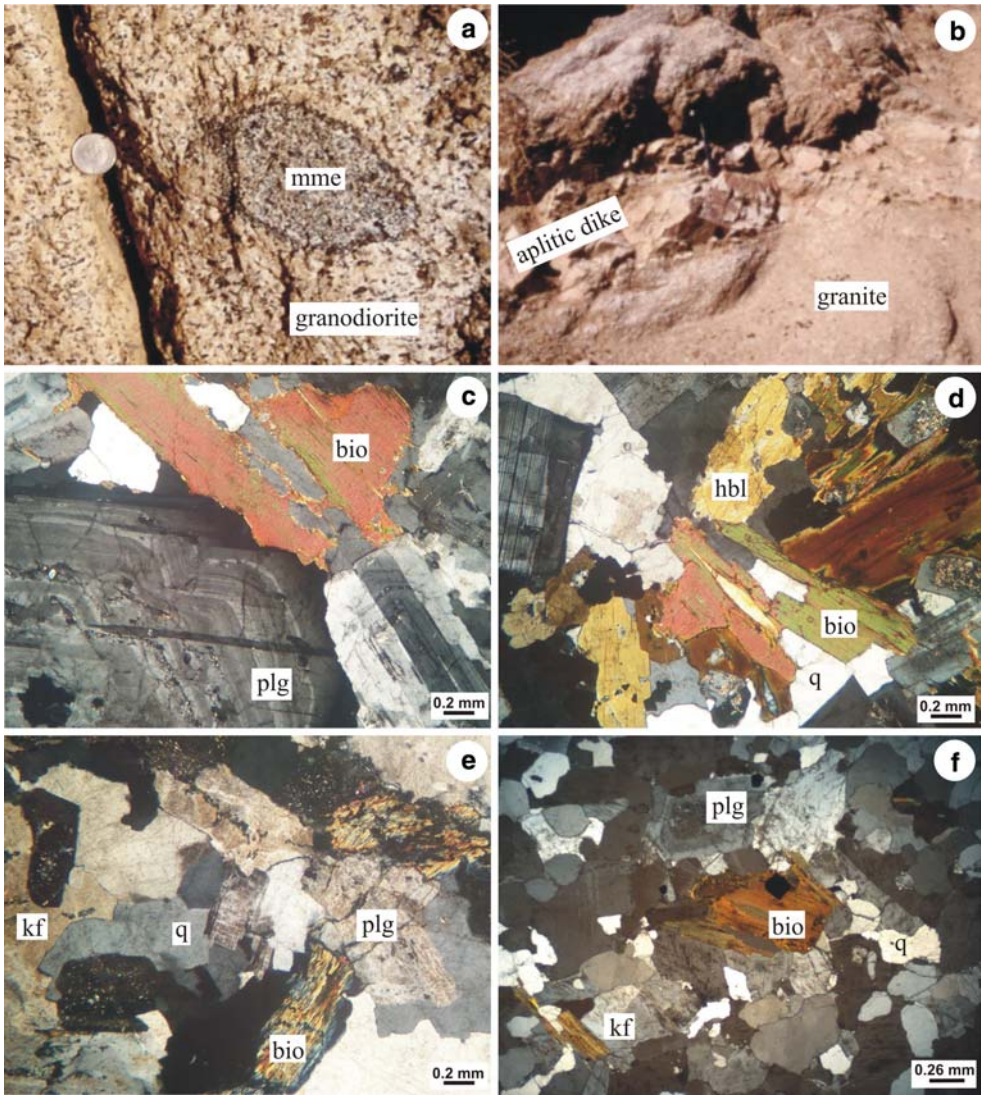

Fig. 6 Field and microscopic views from the granitoid rocks. Abbreviations: *mme* mafic microgranular enclave, *bio* biotite, *plg* plagioclase, *hbl* hornblende, *kf* K-feldspar, *q* quartz

high Fe^{+2} (1.04) content in the rims (Table 2). Amphibole is a common igneous mineral in hydrous calc-alkalic magmas crystallizing at depth. The chemistry of a crystallizing amphibole is sensitive to pressure, temperature, oxygen fugacity and water fugacity (Spear 1981; Johnson and Rutherford 1989). It has been shown that there is an empirical correlation between the estimated pressures of crystallization of calc-alkaline plutons and the total Al content of hornblende (Hammarstrom and Zen 1986; Hollister et al. 1987; Johnson and Rutherford 1989; Schmidt 1992). The analysed hornblendes from the granodiorite samples yielded pressures, ranging from 0.79 to 3.81 kbar based on the equation of Hammarstrom and Zen (1986), ranging from 0.52 to 3.9 kbar based on the equation of Hollister et al. (1987), 0.50–3.04 kbar based on the equation of Johnson and Rutherford (1989), 1.45–4.3 kbar based on the equation of Schmidt (1992). When combined, the average Al geobarometer is between 0.82 and 3.76 kbar. These values correspond to depths ranging from 3 to 10 km. This may indicate that the early phases of the granitoids started to crystallize at relatively great depth and that final crystallization occurred at shallower levels during uplift of the granitoid body.

The biotite is a common hydrated ferromagnesian silicate in mafic, intermediate and felsic igneous rocks. It is a very sensitive indicator of physico-chemical conditions and compositional evolution in granitoid genesis (Speer 1984). Hence, there is a relation between the compositions of igneous biotites and their host magmas (Abdel-Rahman 1994). The Al_2O_3,MgO and FeO contents of the biotites were used to discriminate anorogenic alkaline, peraluminous (including S-type) and calcalkaline suites in granitoid rocks (Abdel-Rahman 1994). The Al_2O_3 content of the biotites in the granodiorites from the Göksun–Afşin (Kahramanmaraş) region ranges from 13.51 to 14.69%; the MgO content ranges from 11.85 to 14.38%, and the FeO content ranges from 17.17 to 19.86% (Table 3). The MgO–FeO*–Al_2O_3 triangular and the Al_2O_3 versus MgO diagram clearly show that the biotites from the rocks studied plot within the field of calc-alkaline orogenic suites (Fig. 7c, d). The

Table 1 Mineral chemistry of the feldspar minerals from the granodiorite rocks

Sample	Plagioclase										K-feldspar					
	K199-4c	K199-4r	K199-5c	K199-5r	K201-5	K201-7	K39-3	K39-11	K204-7	K204-18	K199-1	K199-3	K201-1	K204-1	K204-4	K39-1
SiO_2	58.35	56.40	54.05	61.80	63.61	55.63	53.37	63.35	51.55	66.28	65.36	66.36	65.59	65.35	64.22	65.38
Al_2O_3	26.19	26.16	29.22	24.13	22.67	28.00	29.63	22.70	31.00	21.56	18.14	17.95	17.93	18.58	18.27	18.43
TiO_2	0.01	0.01	0.01	0.03	0.00	0.00	0.00	0.01	0.01	0.00	0.05	0.00	0.08	0.01	0.03	0.00
FeO*	0.24	0.20	0.18	0.17	0.18	0.15	0.30	0.16	0.18	0.02	0.10	0.06	0.10	0.08	0.01	0.05
MnO	0.00	0.00	0.00	0.00	0.00	0.00	0.03	0.00	0.01	0.00	0.01	0.00	0.02	0.00	0.02	0.00
MgO	0.02	0.01	0.02	0.01	0.00	0.00	0.01	0.02	0.00	0.00	0.00	0.00	0.00	0.01	0.00	0.00
CaO	8.74	9.24	12.28	6.15	4.44	10.28	11.80	3.90	13.46	2.30	0.04	0.00	0.08	0.05	0.06	0.05
Na_2O	6.40	5.83	4.38	7.86	8.97	5.65	4.39	9.19	3.59	10.14	1.53	0.79	1.57	1.50	0.32	2.01
K_2O	0.23	0.19	0.08	0.33	0.35	0.13	0.17	0.33	0.13	0.18	13.70	14.91	13.43	14.64	16.17	13.78
Total	100.18	98.02	100.22	100.47	100.23	99.84	99.71	99.66	99.92	100.47	98.93	100.07	98.79	100.23	99.10	99.70
Si	2.62	2.59	2.45	2.74	2.81	2.51	2.43	2.81	2.35	2.91	3.04	3.07	3.06	3.00	3.00	3.01
Al	1.38	1.42	1.56	1.26	1.18	1.49	1.59	1.19	1.66	1.11	1.04	1.05	1.05	1.00	1.00	1.01
Ti	0.00	0.00	0.00	0.00	0.00	0.00	0.00	0.00	0.00	0.00	0.00	0.00	0.00	0.00	0.00	0.00
Fe^{2+}	0.01	0.01	0.01	0.01	0.01	0.01	0.01	0.01	0.01	0.00	0.00	0.00	0.00	0.00	0.00	0.00
Mn	0.00	0.00	0.00	0.00	0.00	0.00	0.00	0.00	0.00	0.00	0.00	0.00	0.00	0.00	0.00	0.00
Mg	0.00	0.00	0.00	0.00	0.00	0.00	0.00	0.00	0.00	0.00	0.00	0.00	0.00	0.00	0.00	0.00
Ca	0.42	0.45	0.60	0.29	0.21	0.50	0.57	0.19	0.66	0.11	0.00	0.00	0.00	0.00	0.00	0.00
Na	0.56	0.52	0.38	0.68	0.77	0.49	0.39	0.79	0.32	0.86	0.14	0.07	0.14	0.13	0.03	0.18
K	0.01	0.01	0.00	0.02	0.02	0.01	0.01	0.02	0.01	0.01	0.81	0.88	0.80	0.86	0.96	0.81
Total	5.00	5.00	5.00	5.00	5.00	5.00	5.00	5.00	5.00	5.00	5.00	5.00	5.00	5.00	5.00	5.00
Or	1.33	1.15	0.45	1.92	1.99	0.72	1.01	1.89	0.77	1.02	85.29	92.53	84.54	86.28	96.76	81.66
Ab	56.24	52.69	39.08	68.48	76.96	49.51	39.82	79.47	32.32	87.96	14.50	7.47	15.06	13.45	2.94	18.07
An	42.43	46.15	60.47	29.60	21.05	49.77	59.17	18.64	66.91	11.02	0.21	0.00	0.40	0.27	0.30	0.27

Number of ions on the basis of eight oxygens. Total Fe is expressed as FeO*, c and r represent core and rim, respectively

FeO*/MgO ratio varies between 1.44 and 1.67 (Table 3), similar to the average ratio (1.76) of subduction related calc-alkaline magmas (Abdel-Rahman 1994).

Geochemistry

Major, trace and rare earth element contents of the granitoid rocks from the Göksun and Afşin (Kahramanmaraş) region are presented in Table. 4 and 5. Compared to granites and aplitic dikes, the granodiorites are characterized by high TiO_2 (0.25–0.46 wt %), Al_2O_3 (15.01–16.45 wt %), FeO (2.58–5.64 wt %), MgO (0.82–2.25 wt %), CaO (1.74–5.04 wt %), P_2O_5 (0.09–0.13 vol. %), Zr (84–138 ppm) and Sr (185–395 ppm) contents and low SiO_2 (63.8–69.7 wt %) and K_2O (2.36–4.54 wt %) contents (Table. 4, 5). In Harker's (1909) variation diagrams, the granodiorites, granites and aplitic dikes define a coherent trends. This may simply be explained by fractional crystallization. The Al_2O_3, TiO_2, FeO, MgO, CaO and P_2O_5 contents decrease with increasing SiO_2 contents whereas the K_2O contents increase with increasing SiO_2 (Fig. 8). These variations indicate that plagioclase, hornblende and magnetite crystallizations have played important role during the crystallization of the granitoid rocks. The granitoid rocks in the Göksun–Afşin (Kahramanmaraş) region exhibit a typical calc-alkaline trend on AFM diagram of Irvine and Baragar (1971) (Fig. 9a). The aluminum saturation index [$Al_2O_3/CaO + Na_2O + K_2O$] of the rocks is presented in Fig. 9b. The granodiorites exhibit metaluminous (A/CNK = 0.94) to a peraluminous (A/CNK = 1.09) character whereas the granites and aplitic dikes display peraluminous (A/CNK = 0.99–1.12) character as the rocks become more felsic (Maniar and Piccolli 1989). The REE patterns of the granitoid rocks in Göksun–Afşin (Kahramanmaraş) region are presented in Fig. 10a. All the samples show LREE enrichment and flat HREE patterns [$(La/Lu)_N = 11.75$–5.47 for granodiorites, $(La/Lu)_N = 3.34$–3.49 for granites and $(La/Lu)_N = 4.66$–0.49 for aplitic dikes], and also a marked negative Eu anomalies indicative of feldspar involvement during fractionation and/or melting (Rollinson 1993). The REE patterns of the rocks studied show similarities to granitoids of modern arc settings (Pearce et al. 1984). The Ocean ridge granite (ORG)-normalized multi element diagram of the granitoids display selective enrichment in large ion lithophile (LIL) elements such as Rb, Ba, Th and depletion in high field strength (HFS) elements such as Ta, Nb, Zr, Hf, Sm, Y, Yb (Fig. 10b). The field of plutons from modern volcanic arc settings is shown for comparison (Pearce et al. 1984). The multi-element patterns of the granitoid rocks show similarity to volcanic arc granites (Fig. 10b). Moreover distinctly negative Nb anomaly are typical of magmas derived from a subduction-metasomatized mantle (Wilson 1989). Tectonomagmatic discrimination diagrams of Pearce et al. (1984) based on immobile elements are effective at discriminating between tectonic environments in granitoid material. Figure 11 presents Nb versus Y and Rb versus Y + Nb diagrams for the granitoid rocks from Göksun–Afşin (Kahramanmaraş) region. The Nb versus Y diagram separates volcanic arc + syncollisional

Table 2 Mineral chemistry of the amphibole mineral from the granodiorite rocks

Sample	Amphibole																		
	K199-1	K199-2	K199-3c	K199-3r	K199-4	K201-1	K201-2	K201-3	K201-4	K204-1	K204-3	K204-4	K204-5	K204-6	K204-7	K204-8	K204-11	K204-12	K204-14
SiO_2	48.43	48.01	48.53	48.74	51.33	46.60	48.28	49.20	47.91	46.38	47.44	49.55	49.32	49.22	45.00	45.31	47.14	47.05	50.93
TiO_2	0.94	1.52	1.60	0.88	0.54	1.49	0.77	0.58	0.89	0.90	0.89	0.64	0.61	0.65	1.17	1.18	0.91	0.90	0.17
Al_2O_3	7.30	7.96	7.33	6.99	4.60	8.37	7.06	7.09	7.01	8.04	7.07	5.86	5.52	5.55	8.79	8.75	7.43	7.39	4.92
Cr_2O_3	0.00	0.00	0.00	0.02	0.00	0.02	0.00	0.00	0.00	0.00	0.02	0.01	0.02	0.00	0.03	0.02	0.00	0.04	0.01
FeO	15.27	14.43	13.54	15.72	14.42	14.14	15.53	15.08	15.88	16.82	16.01	14.19	14.42	14.25	16.94	17.20	16.41	16.22	14.45
MnO	0.55	0.41	0.32	0.70	0.73	0.46	0.67	0.59	0.73	0.68	0.70	0.67	0.68	0.72	0.71	0.66	0.68	0.70	0.64
MgO	13.09	13.54	14.28	13.04	14.50	13.38	12.77	12.92	12.59	11.82	12.48	13.99	14.31	14.22	11.18	11.27	12.28	12.41	14.03
CaO	11.16	10.83	10.84	11.18	11.44	10.93	10.97	11.37	11.34	11.29	11.32	11.37	11.34	11.33	11.30	11.25	11.30	11.22	11.89
Na_2O	1.28	1.53	1.26	1.13	0.81	1.60	1.12	1.07	1.13	1.11	1.10	0.93	0.86	0.88	1.41	1.46	1.15	1.14	0.62
K_2O	0.57	0.47	0.51	0.51	0.37	0.54	0.67	0.32	0.49	0.64	0.65	0.44	0.44	0.44	0.75	0.72	0.56	0.57	0.24
Total	98.59	98.70	98.21	98.91	98.75	97.52	97.84	98.23	97.98	97.69	97.68	97.65	97.53	97.26	97.28	97.82	97.86	97.65	97.92
Si	6.96	6.85	6.91	6.98	7.30	6.75	6.99	7.08	6.96	6.79	6.93	7.14	7.10	7.11	6.67	6.67	6.87	6.86	7.32
Al	1.04	1.15	1.09	1.02	0.70	1.25	1.01	0.92	1.04	1.21	1.07	0.86	0.90	0.89	1.33	1.33	1.13	1.14	0.68
Al	0.19	0.19	0.14	0.16	0.07	0.18	0.20	0.28	0.16	0.18	0.14	0.13	0.04	0.06	0.21	0.19	0.15	0.13	0.16
Fe(III)	0.75	0.82	0.85	0.84	0.75	0.81	0.80	0.66	0.75	0.86	0.76	0.74	0.90	0.86	0.73	0.77	0.83	0.87	0.60
Ti	0.10	0.16	0.17	0.09	0.06	0.16	0.08	0.06	0.10	0.10	0.10	0.07	0.07	0.07	0.13	0.13	0.10	0.10	0.02
Cr	0.00	0.00	0.00	0.00	0.00	0.00	0.00	0.00	0.00	0.00	0.00	0.00	0.00	0.00	0.00	0.00	0.00	0.00	0.00
Fe(II)	1.09	0.90	0.76	1.04	0.97	0.90	1.08	1.16	1.18	1.20	1.19	0.97	0.83	0.86	1.37	1.35	1.18	1.11	1.14
Mn	0.07	0.05	0.04	0.08	0.09	0.06	0.08	0.07	0.09	0.08	0.09	0.08	0.08	0.09	0.09	0.08	0.08	0.09	0.08
Mg	2.80	2.88	3.03	2.78	3.07	2.89	2.76	2.77	2.73	2.58	2.72	3.01	3.07	3.06	2.47	2.47	2.67	2.70	3.01
Ca	1.72	1.66	1.65	1.71	1.74	1.70	1.70	1.75	1.76	1.77	1.77	1.75	1.75	1.75	1.79	1.77	1.76	1.75	1.83
Na	0.36	0.42	0.35	0.31	0.22	0.45	0.31	0.30	0.32	0.31	0.31	0.26	0.24	0.25	0.40	0.42	0.32	0.32	0.17
K	0.10	0.09	0.09	0.09	0.07	0.10	0.12	0.06	0.09	0.12	0.12	0.08	0.08	0.08	0.14	0.14	0.10	0.11	0.04
Total	15.18	15.17	15.09	15.12	15.03	15.24	15.14	15.11	15.17	15.21	15.20	15.10	15.07	15.08	15.34	15.33	15.19	15.18	15.05
Mg#	0.72	0.76	0.80	0.73	0.76	0.76	0.72	0.71	0.70	0.68	0.69	0.76	0.79	0.78	0.64	0.65	0.69	0.71	0.73

Number of ions on the basis of 23 oxygens. Total Fe is expressed as FeO*, c and r represent core and rim, respectively

Table 3 Mineral chemistry of the biotite mineral from the granodiorite rocks

Sample	Biotite																	
	K199-1c	K199-1r	K199-2c	K199-2r	K201-1	K201-5c	K201-5r	K201-9	K39-1	K39-3	K39-5	K39-7	K204-8	K204-13	K204-14	K204-15	K204-16	K204-20
SiO_2	37.28	37.47	37.58	37.44	37.76	37.78	37.53	37.38	36.75	37.18	37.01	36.63	37.57	36.67	36.61	36.62	36.71	37.11
TiO_2	3.77	3.45	3.67	3.81	3.59	3.31	3.41	3.37	3.68	3.65	3.68	3.61	2.99	3.64	3.65	3.84	3.84	2.99
Al_2O_3	13.58	13.73	13.59	13.78	13.68	13.94	14.04	14.16	14.14	14.29	14.02	14.20	13.85	14.02	14.01	14.13	13.96	14.18
FeO	19.47	19.03	19.34	19.14	18.98	19.41	19.50	19.49	18.37	18.43	19.34	18.62	19.15	19.84	19.43	19.74	19.34	19.28
MnO	0.41	0.44	0.37	0.40	0.43	0.40	0.43	0.42	0.60	0.65	0.73	0.66	0.42	0.44	0.40	0.43	0.40	0.50
MgO	12.30	12.52	12.37	12.40	12.45	12.28	12.06	12.16	12.76	12.68	12.02	12.48	12.85	11.91	11.91	12.08	11.95	12.38
CaO	0.00	0.01	0.13	0.18	0.10	0.00	0.03	0.10	0.02	0.01	0.03	0.00	0.02	0.12	0.00	0.01	0.00	0.06
Na_2O	0.13	0.09	0.14	0.09	0.07	0.08	0.07	0.05	0.13	0.10	0.08	0.08	0.09	0.14	0.11	0.13	0.16	0.07
K_2O	8.65	8.98	8.36	7.97	8.46	8.84	8.83	8.32	9.41	9.34	9.18	9.35	9.29	9.26	9.22	9.25	9.16	9.03
Total	95.57	95.71	95.55	95.20	95.52	96.05	95.89	95.45	95.86	96.33	96.08	95.63	96.22	96.02	95.33	96.23	95.53	95.59
Si	5.66	5.68	5.69	5.67	5.71	5.70	5.68	5.67	5.57	5.60	5.62	5.57	5.67	5.58	5.60	5.56	5.60	5.64
Ti	0.43	0.39	0.42	0.43	0.41	0.38	0.39	0.38	0.42	0.41	0.42	0.41	0.34	0.42	0.42	0.44	0.44	0.34
Al(IV)	2.34	2.32	2.31	2.33	2.29	2.30	2.32	2.33	2.43	2.40	2.38	2.43	2.33	2.42	2.40	2.44	2.40	2.36
Al(VI)	0.09	0.13	0.12	0.14	0.15	0.18	0.18	0.20	0.10	0.14	0.12	0.12	0.14	0.10	0.13	0.09	0.11	0.19
Fe^{2+}	2.47	2.41	2.45	2.43	2.40	2.45	2.47	2.47	2.33	2.32	2.45	2.37	2.42	2.53	2.49	2.51	2.47	2.45
Mn	0.05	0.06	0.05	0.05	0.06	0.05	0.06	0.05	0.08	0.08	0.09	0.09	0.05	0.06	0.05	0.06	0.05	0.06
Mg	2.79	2.83	2.79	2.80	2.81	2.76	2.72	2.75	2.89	2.85	2.72	2.83	2.89	2.70	2.71	2.73	2.72	2.81
Ca	0.00	0.00	0.02	0.03	0.02	0.00	0.00	0.01	0.00	0.00	0.00	0.00	0.00	0.02	0.00	0.00	0.00	0.01
Na	0.04	0.03	0.04	0.03	0.02	0.02	0.02	0.02	0.04	0.03	0.02	0.02	0.03	0.04	0.03	0.04	0.05	0.02
K	1.68	1.74	1.62	1.54	1.63	1.70	1.70	1.61	1.82	1.80	1.78	1.81	1.79	1.80	1.80	1.79	1.78	1.75
OH	0.00	0.00	0.00	0.00	0.00	0.00	0.00	0.00	0.00	0.00	0.00	0.00	0.00	0.00	0.00	0.00	0.00	0.00
Total	15.55	15.58	15.50	15.44	15.49	15.55	15.54	15.50	15.67	15.63	15.61	15.66	15.66	15.66	15.63	15.65	15.62	15.63
Mg#	0.53	0.54	0.53	0.54	0.54	0.53	0.52	0.53	0.55	0.55	0.53	0.54	0.54	0.52	0.52	0.52	0.52	0.53
FeO*/MgO	1.58	1.52	1.56	1.54	1.52	1.58	1.62	1.60	1.44	1.45	1.61	1.49	1.49	1.67	1.63	1.63	1.62	1.56

Number of ions on the basis of 22 oxygens. Total Fe is expressed as FeO*, c and r represent core and rim, respectively

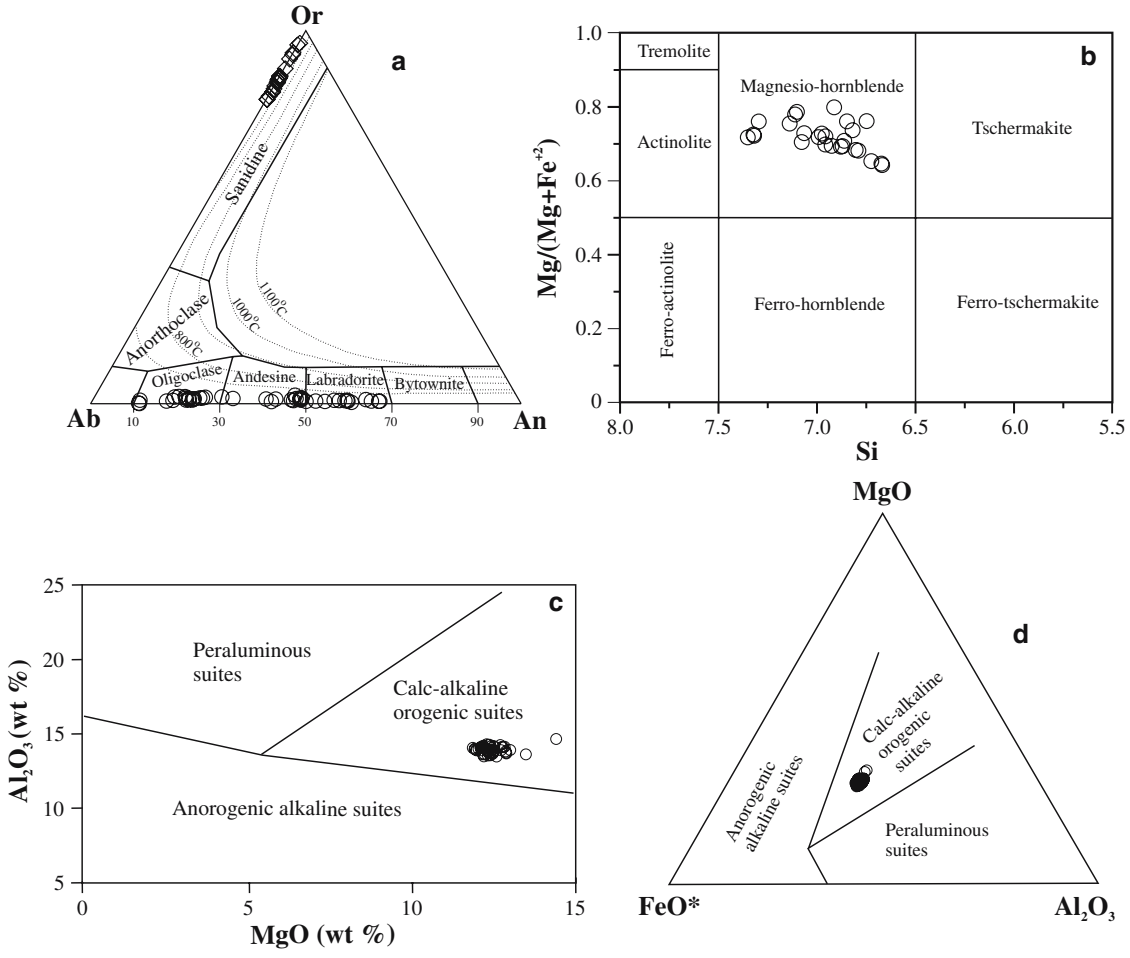

Fig. 7 **a** Classification of feldspars (*circle* is plagioclase and *diamond* is K-feldspar), **b** classification of amphibole (after Leake et al. 1997), **c** MgO versus Al_2O_3 and **d** FeO–Al_2O_3–MgO ternary diagram for the biotite (after Abdel-Rahman 1994)

and within plate granites (Fig. 11a). The samples from this study are mainly plotted in the volcanic arc + syncollisional granite field. To separate volcanic arc granites from syncollisional granites, a Rb versus Y + Nb diagram is used in Fig. 11b. It is clear that the granitoid rocks of the study area plot within the volcanic arc granite field. A subset of selected samples were analysed by ICP-MS. These samples are used within the Rb–Hf–Ta triangular diagram of Harris et al. (1986) which discriminates volcanic arc, ocean floor and within-plate type granitoids (Fig. 12a). The granitoid rocks of the Göksun–Afşin (Kahramanmaraş) region are characterized by Ta depletion and plot within the volcanic arc field. Brown et al. (1984) stated that the Rb/Zr ratio increases with increasing Nb content in accordance with the arc maturity. Once it is well constrained that the granitoid rocks of the study area were formed in a volcanic arc setting one may compare the data with the field of arc-type granitoids (Fig. 12b): they mainly overlap in the field of normal continental arc and are also slightly transitional to the field of mature arc.

K–Ar geochronology

Thirteen (12 biotite and 1 hornblende separates) samples from the granodiorite and one sample (biotite separate) from the aplitic dike cutting the granites have been used for K–Ar isotopic age determination (Table 6). No granite samples were included for K–Ar isotopic dating due to low-temperature alteration effects on the biotite and hornblende. As the proportion of radiogenic to total ^{40}Ar increases, it is evident that the error in its measurement decreases exponentially (Cox and Dalrymple 1967). Except for sample K-36, the radiogenic $^{40}Ar^*$ in the measured biotite and hornblende separates ranges from 92.8 to 66.7% (Table 6). The biotite ages from the granodiorite samples cluster in two groups. The first group ranges from 74.40 ± 1.5 to 70.05 ± 1.75 Ma, whereas the second group ranges from 80.42 ± 2.0 to 77.49 ± 1.91 Ma (Table 6). The petrography of the samples dated in the first group show that the biotites exhibit slight effects of chlorite alteration which may reduce the ages. It is known that chemical weathering

Table 4 Major and trace element analyses of the granitoid rocks from Göksun–Afşin (Kahramanmaraş) region, SE Turkey

Samples	Granodiorite																	Granite						
	K-36	K-37	K-38	K-39	K-171	K-172	K-173	K-198	K-199	K-200	K-201	K-202	K-203	K-204	K-205	K-206	K-207	K-40	K-41	K-42	K-43	K-44	K-45	K-46
SiO_2	68.64	69.00	68.37	69.74	66.28	64.03	64.41	63.82	63.98	64.38	65.05	64.15	64.64	65.68	68.26	67.94	69.39	76.78	75.89	75.80	75.94	75.92	75.70	75.69
TiO_2	0.30	0.30	0.33	0.25	0.37	0.36	0.37	0.46	0.44	0.43	0.40	0.43	0.42	0.42	0.33	0.33	0.30	0.05	0.05	0.05	0.05	0.05	0.05	0.05
Al_2O_3	15.61	15.52	15.90	15.40	15.19	15.97	15.38	16.04	16.45	16.01	16.41	16.37	16.20	16.02	15.66	15.32	15.01	13.05	13.17	13.32	13.31	13.34	13.48	13.65
FeO*	3.02	3.06	3.21	2.58	4.57	4.80	4.75	5.64	5.32	5.07	5.07	5.24	5.26	4.87	2.88	3.67	3.29	0.46	0.84	0.96	0.76	0.75	0.63	0.72
MnO	0.06	0.04	0.06	0.05	0.05	0.07	0.05	0.10	0.10	0.09	0.09	0.09	0.10	0.09	0.07	0.06	0.04	0.02	0.01	0.00	0.01	0.01	0.00	0.02
MgO	1.03	0.99	1.04	0.82	1.90	2.11	1.98	2.25	2.17	2.02	1.82	2.00	1.97	1.98	1.15	1.24	1.01	0.10	0.08	0.07	0.09	0.09	0.08	0.11
CaO	2.99	2.55	3.43	2.80	3.06	1.74	1.94	4.94	5.04	4.88	4.83	4.92	4.96	4.85	3.77	3.27	2.80	0.56	0.36	0.46	0.43	0.50	0.31	0.29
Na_2O	3.55	3.28	3.65	3.35	3.70	4.92	4.88	3.13	3.24	3.28	3.37	3.31	3.24	3.19	3.71	3.30	3.04	3.22	3.37	3.77	3.81	3.74	3.36	3.39
K_2O	3.43	3.93	3.00	3.96	2.86	3.30	3.08	2.55	2.49	2.49	2.52	2.56	2.36	2.40	3.41	3.85	4.54	4.94	5.63	5.00	4.70	5.11	5.70	5.49
P_2O_5	0.11	0.10	0.11	0.09	0.12	0.13	0.12	0.11	0.10	0.11	0.11	0.11	0.11	0.11	0.10	0.11	0.10	0.05	0.04	0.04	0.03	0.04	0.04	0.03
LOI	0.85	0.66	0.50	0.43	2.14	2.17	2.51	0.59	0.53	0.55	0.39	0.49	0.67	0.61	0.45	0.50	0.36	0.44	0.16	0.14	0.59	0.35	0.28	0.38
Total	99.59	99.43	99.61	99.46	100.24	99.60	99.47	99.63	99.86	99.31	100.05	99.67	99.93	100.21	99.80	99.60	99.87	99.66	99.60	99.62	99.71	99.90	99.63	99.81
Nb	8	9	11	9	7	8	8	6	6	7	7	6	6	7	13	10	10	15	17	18	19	17	20	16
Zr	135	135	138	129	125	126	133	94	84	84	86	97	84	108	117	123	107	50	35	43	43	34	47	43
Y	17	16	19	17	26	28	27	21	17	19	18	20	18	21	22	23	24	8	20	33	33	22	36	24
Sr	243	209	226	218	395	286	244	224	236	221	227	225	233	222	203	192	185	49	18	15	15	14	16	18
U	4	5	7	6	10	8	10	3	2	3	2	3	3	6	6	5	3	6	8	6	6	4	6	4
Rb	123	137	124	149	92	104	100	90	86	88	89	90	97	94	112	139	143	197	121	123	120	114	153	140
Th	19	31	27	32	29	33	29	10	9	9	4	10	6	10	18	18	13	38	21	33	30	32	30	31
Pb	30	25	25	29	64	22	55	11	10	9	10	11	10	12	13	15	13	40	53	39	42	47	50	38
Ga	20	21	21	22	15	18	17	16	15	19	17	18	17	15	17	18	17	19	20	20	21	20	20	21
Ni	3	2	2	2	7	7	6	6	8	5	5	8	5	4	3	3	5	2	2	2	2	2	2	2
Co	4	4	6	3	13	11	7	10	11	10	12	12	12	11	5	6	6	2	2	2	2	2	2	2
Cr	6	5	7	11	29	198	20	20	198	20	25	24	21	17	23	11	36	2	5	7	4	2	2	5
V	41	45	44	38	105	105	100	99	91	107	95	88	97	95	49	56	46	7	4	5	4	4	6	7
Ba	701	838	606	907	1,098	1,345	1,087	614	570	607	595	578	558	523	740	739	775	219	85	61	80	49	86	158
Hf	7	6	7	6	7	6	6	3	6	5	4	7	7	6	6	6	6	5	5	5	6	5	6	5
Sc	6	6	7	6	15	15	16	20	18	20	16	13	16	17	14	15	7	2	2	2	2	2	2	2

Table 4 (Contd.)

Samples	Granite								Aplitic dike													
	K-47	K-163	K-164	K-165	K-166	K-167	K-168	K-169	K-184	K-185	K-186	K-187	K-188	K-189	K-190	K-191	K-192	K-193	K-194	K-195	K-196	K-197
SiO_2	74.16	76.57	76.82	76.82	77.06	76.19	75.82	75.89	76.53	76.02	76.20	76.12	76.41	76.54	75.52	76.67	75.68	76.86	76.47	76.14	77.07	75.53
TiO_2	0.10	0.05	0.06	0.07	0.06	0.08	0.09	0.08	0.05	0.07	0.04	0.04	0.04	0.06	0.04	0.04	0.04	0.03	0.03	0.03	0.05	0.04
Al_2O_3	12.62	13.02	12.88	12.88	12.78	12.30	12.84	12.83	12.98	13.21	12.68	13.06	13.28	13.02	12.97	13.20	13.36	12.47	13.36	13.32	12.79	13.08
FeO*	1.55	0.69	0.68	1.18	0.81	1.41	1.31	1.32	1.09	1.25	0.74	0.77	0.85	0.68	0.58	0.78	0.76	0.48	0.76	0.83	0.78	0.91
MnO	0.05	0.01	0.01	0.01	0.01	0.01	0.01	0.01	0.04	0.05	0.03	0.03	0.02	0.02	0.03	0.03	0.05	0.02	0.03	0.03	0.02	0.04
MgO	0.29	0.06	0.06	0.11	0.15	0.23	0.23	0.21	0.12	0.18	0.03	0.07	0.13	0.09	0.04	0.06	0.05	0.02	0.05	0.06	0.11	0.05
CaO	2.06	0.94	0.92	1.56	0.97	1.00	1.08	0.96	0.76	0.94	0.63	0.66	0.40	0.65	0.58	0.61	0.50	0.56	0.56	0.62	0.61	0.66
Na_2O	3.19	2.58	2.57	2.72	2.57	2.47	2.35	2.30	3.20	3.23	3.66	3.43	2.89	3.26	3.41	3.69	3.31	4.11	3.75	3.63	3.16	3.89
K_2O	3.29	5.88	5.91	4.77	5.75	5.06	5.96	6.19	5.27	5.03	4.91	5.39	4.79	4.94	5.62	4.99	5.66	4.47	5.07	5.20	4.64	4.70
P_2O_5	0.04	0.01	0.02	0.02	0.02	0.02	0.02	0.02	0.03	0.03	0.03	0.03	0.02	0.02	0.03	0.03	0.04	0.03	0.05	0.03	0.02	0.03
LOI	2.29	0.14	0.11	0.09	0.17	0.35	0.21	0.21	0.17	0.21	0.13	0.15	0.93	0.61	0.10	0.12	0.16	0.09	0.15	0.16	0.75	0.11
Total	99.65	99.95	100.03	100.22	100.34	99.11	99.91	100.01	100.24	100.22	99.08	99.75	99.75	99.88	98.92	100.22	99.61	99.13	100.28	100.05	99.99	99.03
Nb	13	12	12	5	5	4	10	8	6	7	7	7	6	8	7	8	11	20	6	12	6	7
Zr	63	62	63	102	60	75	71	70	53	48	50	57	51	58	49	54	44	34	51	53	51	50
Y	36	10	17	11	7	5	18	14	27	23	30	39	21	22	28	33	33	19	31	41	18	27
Sr	44	48	51	81	76	84	89	73	43	57	26	20	36	42	28	27	19	25	29	19	39	25
U	4	13	11	6	5	7	9	8	7	6	6	7	6	8	7	10	8	9	6	8	6	7
Rb	125	133	135	108	136	115	138	151	171	163	239	214	167	171	220	224	266	216	214	202	157	217
Th	22	36	30	29	43	35	45	38	30	30	23	24	33	42	22	30	22	21	24	25	45	29
Pb	38	18	20	25	14	19	19	18	40	39	37	45	27	37	37	35	44	34	34	40	28	34
Ga	18	11	10	10	10	10	12	12	12	12	12	13	12	12	11	13	13	14	12	13	11	13
Ni	2	3	5	2	2	2	5	2	2	2	2	3	2	2	4	2	3	2	3	2	2	5
Co	2	2	2	3	2	2	2	2	3	3	2	2	2	2	2	2	2	2	2	2	2	2
Cr	5	19	9	23	16	17	30	14	10	12	10	9	17	13	12	24	12	20	13	25	18	31
V	11	4	6	8	11	14	16	14	6	9	4	4	6	3	5	4	6	8	5	6	6	2
Ba	228	451	467	1,437	766	1,879	585	585	224	413	117	78	243	277	128	112	90	133	149	79	283	99
Hf	8	6	8	7	7	7	5	7	7	6	7	7	7	8	5	6	7	6	6	6	7	6
Sc	3	6	3	2	4	2	2	4	2	3	2	2	2	2	2	2	2	2	2	2	4	2

Total Fe is expressed as FeO*

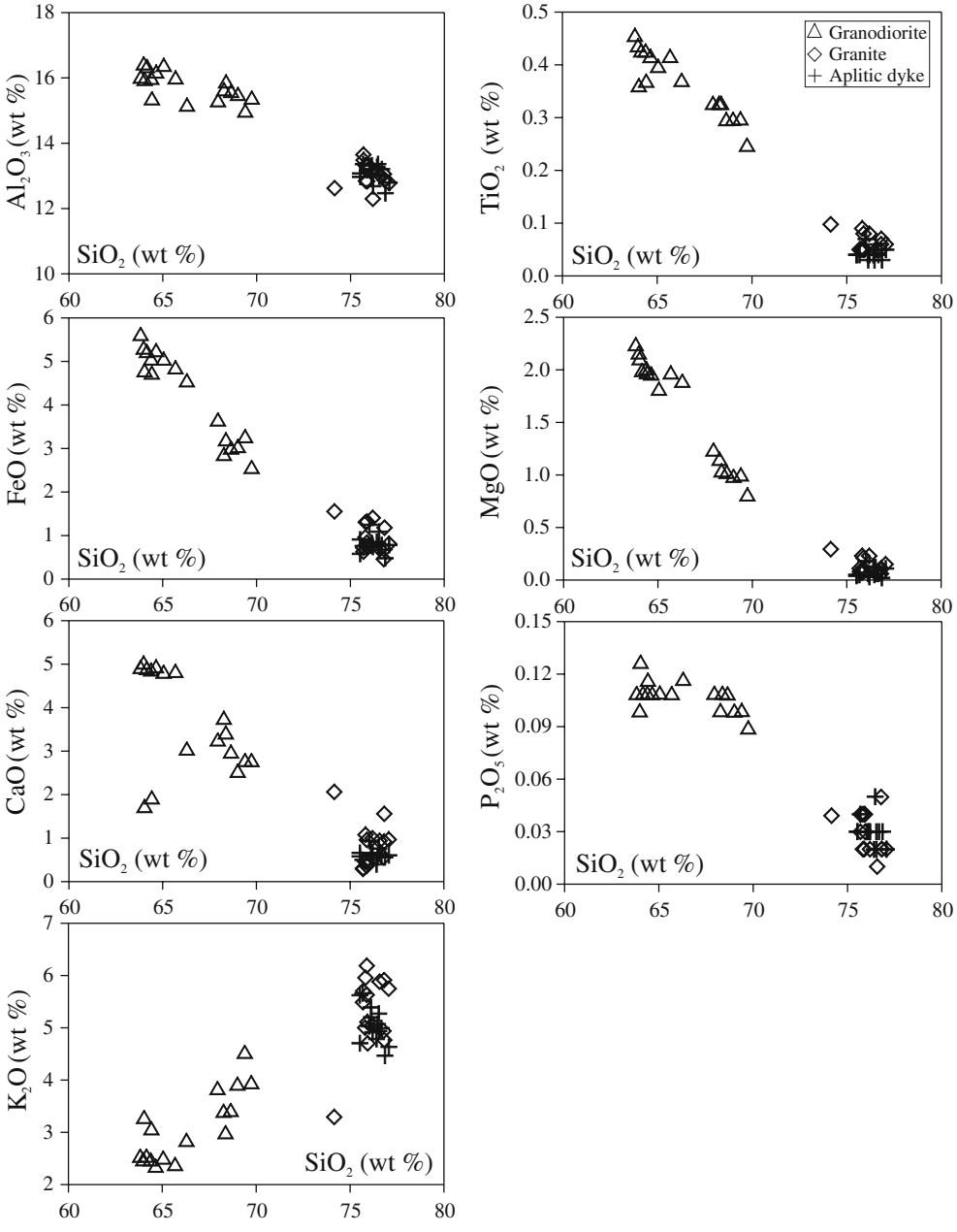

Fig. 8 Harker type (Harker 1909) variation diagrams of the granitoid rocks

and alteration by aqueous fluids lead not only to argon loss but also to changes in the potassium content of minerals (Faure 1986). Therefore, the ages of the first group should be taken with caution. The biotites of the second group are petrographycally fresh and thus are expected to give more reliable ages. The one hornblende separate yielded 85.76 ± 3.17 Ma. (Table 6). The biotite and hornblende ages normally do not provide a measure of the time since the emplacement of a plutonic igneous body, but instead yield information related to the cooling history. The biotite separates from an aplitic dike (K-185) yielded an age of 77.49 ± 1.91 Ma (Table 6). In the field, the aplitic dike is seen to intrude the granites, suggesting that the age of the granite in Göksun–Afşin (Kahramanmaraş) region is coeval or slightly older than the aplitic dikes. All the age determinations from the granitoid rocks in the study area reveal that they were contemporaneously formed during the underthrusting of ophiolitic and related metamorphic units beneath the Malatya–Keban platform in the Late Cretaceous.

Discussion

Three alternative tectonic models have been proposed by several authors to explain genesis and the emplacement of the ophiolites and the granitoid magmatism in the region. These are namely ''single subduction zone'' model (Hall 1976; Aktaş and Robertson 1984, 1990; Yılmaz 1993; Yılmaz et al. 1993; Robertson 1998, 2000), ''double subduction zone'' model (Robertson 1998, 2000, 2002; Parlak et al. 2004) and ''multi-phase

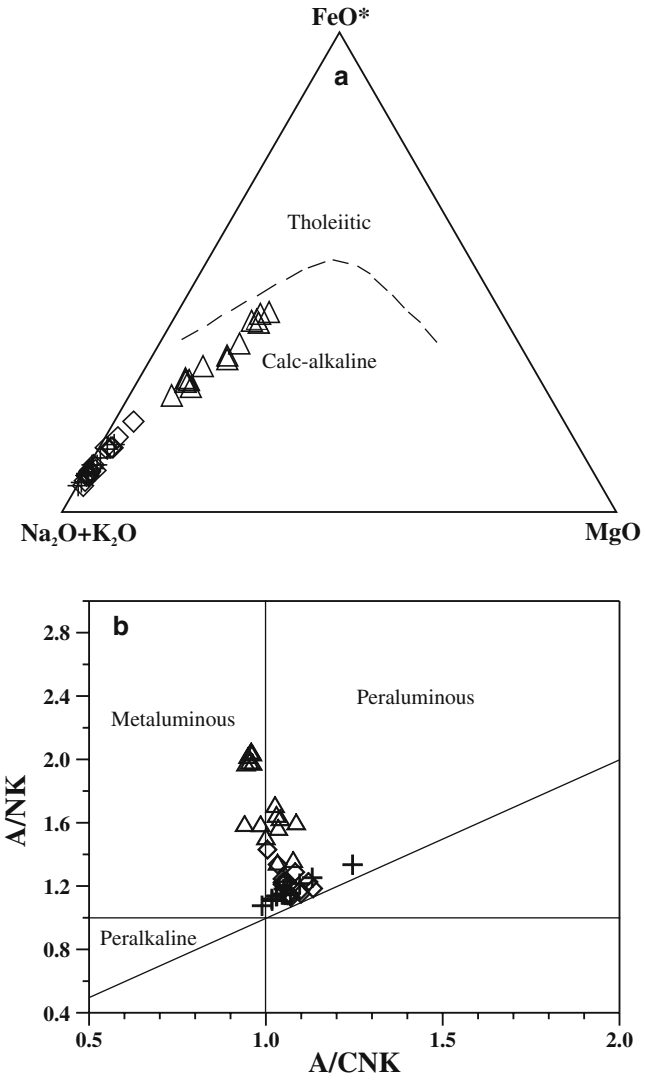

Fig. 9 **a** AFM (after Irvine and Baragar 1971) and **b** A/CNK versus A/NK (after Maniar and Piccolli 1989) diagrams for the granitoid rocks (*triangle* represents granodiorite, *diamond* represents granite and *plus* represents aplitic dike)

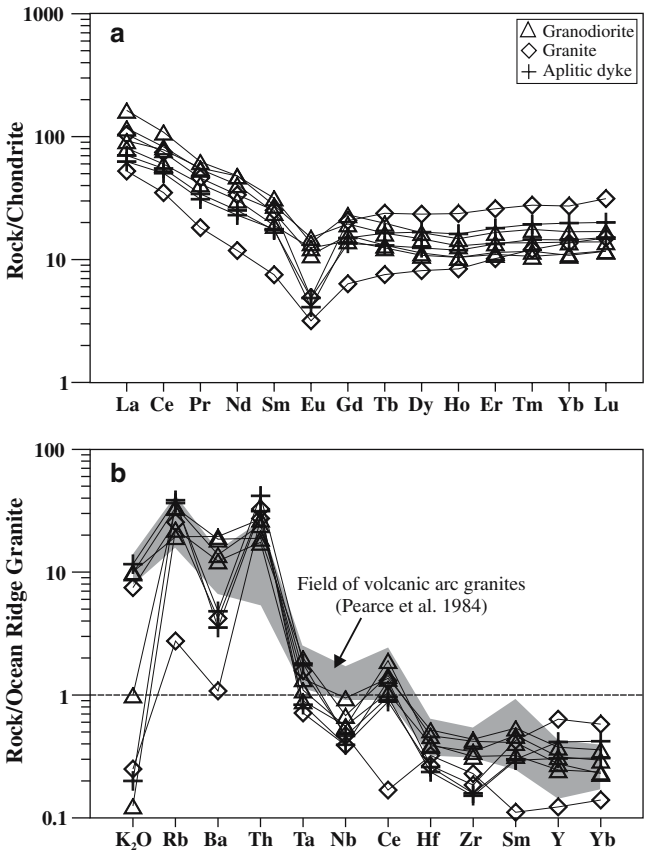

Fig. 10 Chondrite-normalized REE diagram (**a**) and ORG-normalized spider diagram (**b**) of the granitoid rocks (normalizing values are from Sun and McDonough 1989; Pearce et al. 1984)

convergence'' model (Robertson et al. 2006a). The field, geochemical and geochronological data presented here support the ''multi-phase convergence'' model of Robertson et al. (2006a). Before presenting the ''multi-phase convergence'' model, there are number of points which should be clarified. Yazgan and Chessex (1991) and Beyarslan and Bingöl (2000) stated that the Baskil/Elazığ magmatics represent a well-developed magmatic arc unit with plutonic as well as the volcanic rocks. Recent investigations in the region show that the wide spread volcanic units in the region are tholeiitic in character and interpreted as belonging to an ensimatic island arc association which was built up on the top of subduction related oceanic crust (Rızaoğlu et al. 2004; Robertson et al. 2006b). These volcanic units are observed as tectonically overlain by the Malatya–Keban platform and cut by the granitoids in the field, suggesting that the volcanic units were underthrust beneath the Malatya–Keban platform before the granitoid emplacement. The field data also show that the ophiolites and the ophiolite-related metamorphic rocks were accreted to the base of the Malatya–Keban platform before granitoid magmatism (Robertson et al. 2006a). The K–Ar ages obtained from the granitoid of the Göksun–Afşin (Kahramanmaraş) region display an age range from 85 to 77 Ma (Table 6), suggesting that they were formed after the genesis of the ophiolites (~90 Ma) in the southern Neotethys (Mukasa and Ludden 1987; Robertson et al. 2006a).

The wide spread out crops of the granitoids, the ophiolites and the ophiolite-related metamorphic rocks between Kahramanmaraş and Elazığ are important Late Cretaceous tectonomagmatic units of the southeast Anatolian orogen. The granitoids are located in Göksun–Afşin (Kahramanmaraş), Doğanşehir (Malatya) and Baskil (Elazığ) regions (Aktaş and Robertson 1984; Yazgan and Chessex 1991; Beyarslan and Bingöl 2000). They are predominantly composed of plutonic rocks ranging from gabbros to diorites and monzonite. The Late Cretaceous ophiolitic bodies of southeast Anatolia are represented by the Göksun in the north of Kahramanmaraş, İspendere in the Malatya region and Kömürhan-Guleman in the Elazığ region. The ophiolites show a complete ophiolite pseudostratigraphy from the

Table 5 Trace element and REE compositions of the subset of the granitiod rocks analysed by ICP-MS

Sample	Granodiorite				Granite		Aplitic dike	
	K-39	K-171	K-202	K-206	K-47	K-163	K-184	K-196
Th	15.1	21.6	14.0	19.4	26.1	27.7	25.1	33.4
U	5.7	7.66	4.59	4.93	5.47	14.0	5.92	4.82
Nb	6.8	5.5	5.6	9.5	3.9	12.1	3.9	4.6
Hf	4.2	3.5	3.6	4.7	2.4	2.7	2.3	2.1
Ta	1.4	0.77	0.63	0.95	0.5	2.50	0.58	1.26
La	27.8	38.8	19.1	21.9	24.8	12.4	14.9	16.7
Ce	50.5	66.6	36.6	47.9	45.7	21.4	30.9	33.7
Pr	5.15	5.93	3.91	5.28	4.37	1.73	2.95	3.25
Nd	19	22.4	14.2	22.3	15.7	5.53	10.7	11.7
Sm	3.69	4.23	2.90	4.84	3.85	1.15	2.70	2.65
Eu	0.633	0.875	0.721	0.794	0.285	0.184	0.238	0.282
Gd	3.24	4.01	2.91	4.76	4.26	1.31	3.08	2.78
Tb	0.49	0.61	0.47	0.74	0.89	0.28	0.61	0.49
Dy	2.87	3.75	2.75	4.21	5.95	2.07	4.25	3.16
Ho	0.59	0.73	0.59	0.84	1.34	0.48	0.91	0.67
Er	1.89	2.26	1.82	2.75	4.29	1.68	2.98	2.22
Tm	0.298	0.349	0.271	0.448	0.706	0.308	0.494	0.371
Yb	1.84	2.36	1.89	2.86	4.64	2.32	3.37	2.46
Lu	0.297	0.354	0.300	0.430	0.796	0.382	0.510	0.384

ultramafic to volcanic rocks and tectonically underlain by ophiolite-related metamorphic rocks. The ophiolite-related metamorphic rocks crop out discontinuously beneath the ophiolites. The most important one is observed in the Doğanşehir (Malatya) region in tectonic contact with overlying ophiolitic units; they display inverted metamorphic zonation from pyroxene-granulite facies to epidote-amphibolite facies (Genç et al. 1993; Parlak et al. 2002). These ophiolite-related metamorphic rocks is thought to be the equivalent of the Berit metaophiolite (Perinçek and Kozlu 1984; Genç et al. 1993; Robertson et al. 2006a) further to the southwest in the Göksun (Kahramanmaraş) region. K–Ar isotopic age determination on the hornblende yielded an age of 90 ± 7 Ma (Parlak et al. 2002). Figure 13 presents an evolutionary model to explain the genesis of ophiolites and granitoids based on the field, geochemical and geochronological data. The ophiolites in the southeast Anatolia were formed above a north dipping subduction zone between the Arabian platform and the Tauride platform in the Late Cretaceous (~90 Ma) (Parlak et al. 2004) (Fig. 13a). The seamount-type volcanics, MORB type oceanic crust and sea floor sediments occurred during the period between Late Triassic and Early Cretaceous were fragmented and accreted to the base of the hanging wall to form the metaophiolites and/or metamorphic soles in subduction zone (Fig. 13a). An ensimatic island arc was developed above the newly formed subduction-related oceanic crust with time (Fig. 13b). The cold and dense MORB type oceanic crust close to the Tauride platform in the north was then underthrust (Fig. 13b). Following this event the ophiolites and ophiolite-related metamorphic units were then accreted to the base of the Malatya–Keban platform during the progressive subduction of the southern Neotethyan oceanic basin. The thrusting of the Malatya–Keban platform over the ophiolites and the ophiolite-related metamorphic rocks was followed by the intrusion of the

Table 6 K–Ar ages and analytical data for the granodiorite and aplitic dike from the Göksun–Afşin (Kahramanmaraş) region

Sample	Rock type	Mineral	% K	$^{40}Ar^*$ moles/g $\times 10^{-11}$	% $^{40}Ar^*$	$^{40}Ar/^{36}Ar \times 10^2$	$^{40}K/^{36}Ar \times 10^4$	Age (Ma)
K-36	Granodiorite	Biotite	2.35	30.296	46.40	5.51	5.92	72.90 ± 1.70
K-37	Granodiorite	Biotite	4.01	52.023	67.30	9.04	14.00	73.30 ± 1.70
K-38	Granodiorite	Biotite	5.12	66.971	80.40	15.06	27.61	73.90 ± 1.70
K-39	Granodiorite	Biotite	5.01	64.122	66.70	8.88	13.83	72.30 ± 1.60
K-198	Granodiorite	Biotite	5.90	77.720	92.20	37.65	78.62	74.40 ± 1.50
K-200	Granodiorite	Biotite	6.05	78.289	83.63	18.05	34.82	73.12 ± 1.80
K-203	Granodiorite	Biotite	5.50	69.593	76.34	12.49	22.50	71.53 ± 1.77
K-204	Granodiorite	Biotite	5.67	70.228	69.21	9.60	16.01	70.05 ± 1.75
K-198	Granodiorite	Hornblende	0.66	10.006	68.17	9.28	12.40	85.76 ± 3.17
K-199	Granodiorite	Biotite	5.96	83.672	86.93	22.61	41.79	79.19 ± 1.96
K-201	Granodiorite	Biotite	6.17	86.832	89.38	27.83	58.76	79.38 ± 1.97
K-202	Granodiorite	Biotite	6.20	86.243	87.91	24.44	46.10	78.48 ± 1.92
K-206	Granodiorite	Biotite	4.26	60.755	91.08	33.12	63.12	80.42 ± 2.00
K-185	Aplitic dike	Biotite	6.55	89.930	92.80	41.07	82.96	77.49 ± 1.91

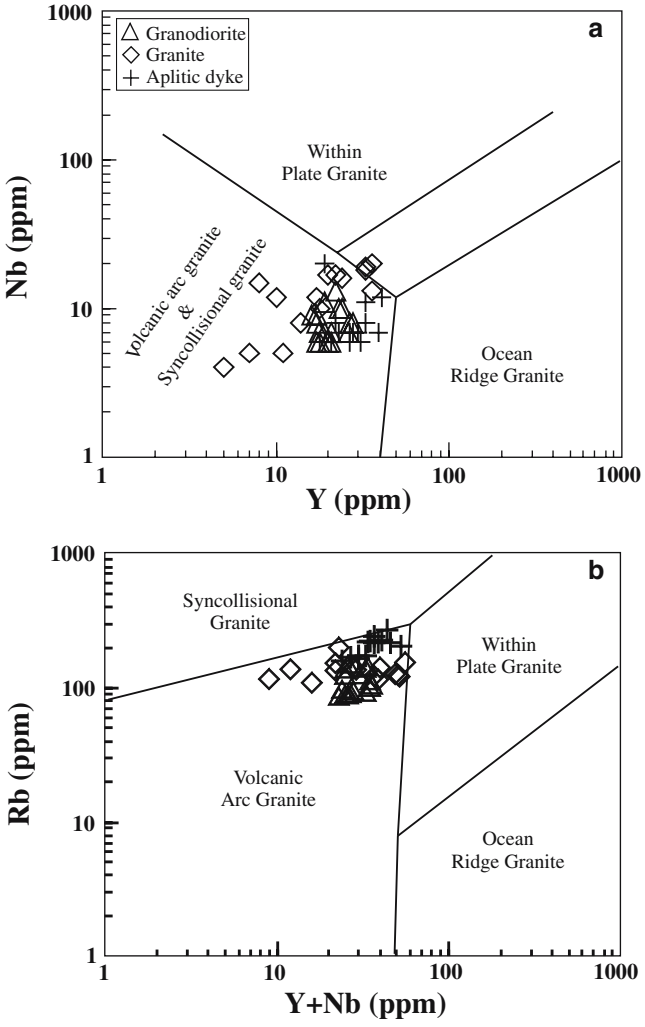

Fig. 11 Tectonomagmatic discrimination diagrams based on Nb versus Y (**a**) and Rb versus Y + Nb (**b**) for the granitoid rocks (after Pearce et al. 1984)

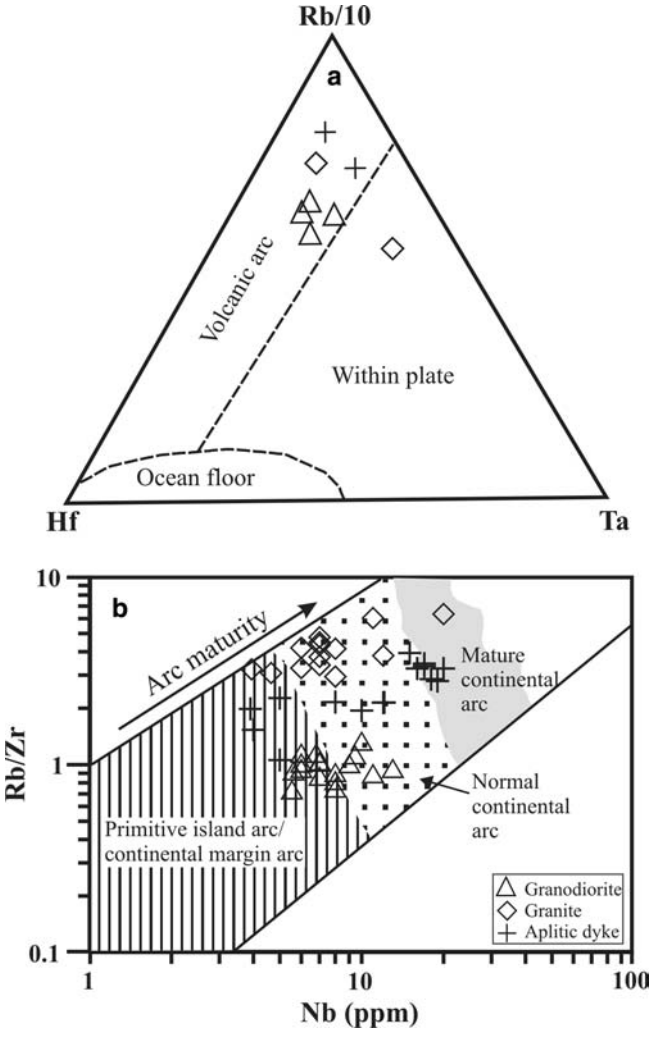

Fig. 12 **a** Rb–Hf–Ta triangular diagram (after Harris et al. 1986) and **b** Rb/Zr versus Nb diagram (after Brown et al. 1984) for the granitoid rocks

granitoids (88–85 Ma) along the Tauride active continental margin in the southern Neotethys (Fig. 13c).

The major and trace element geochemistry of the granitoid rocks in the Göksun–Afşin (Kahramanmaraş) region suggests that they were formed along the Tauride active continental margin during the Late Cretaceous. The metaluminous to peraluminous nature of the granitod rocks is consistent with an evolution involving contamination of mantle-derived magmas by continental crust. The biotite geochemistry further strengthens the interpretation of subduction-related setting for the granitoids in the southeast Anatolia. Volcanic arc granitoids related to subduction of the Neotethys in Turkey are also reported from the Pontide belt (Arslan et al. 2004; Karslı et al. 2004; Boztuğ et al. 2004). Further east along the Neotethyan belt, a similar history of intraoceanic accretion and later marginal arc magmatism of Cretaceous age is recorded in the Kohistan-Karakorum-Himalayas area (Crawford and Searle 1992; Debon et al. 1987; Petterson and Windley 1985; Rolland et al. 2002).

Conclusions

The field, geochemical and geochronological data obtained in this study suggest following conclusions:

1. The granitoids of the Southeast Anatolian Orogen intrude the metamorphic massifs, the ophiolites and the ophiolite-related metamorphic rocks. This further indicate that the ophiolites and the ophiolite-related metamorphic rocks were accreted to the base of the Malatya–Keban platform before intrusion took place.
2. The K–Ar age determinations indicate that the granitoids in the region date the underthrusting of ophiolitic and related-metamorphic units beneath the

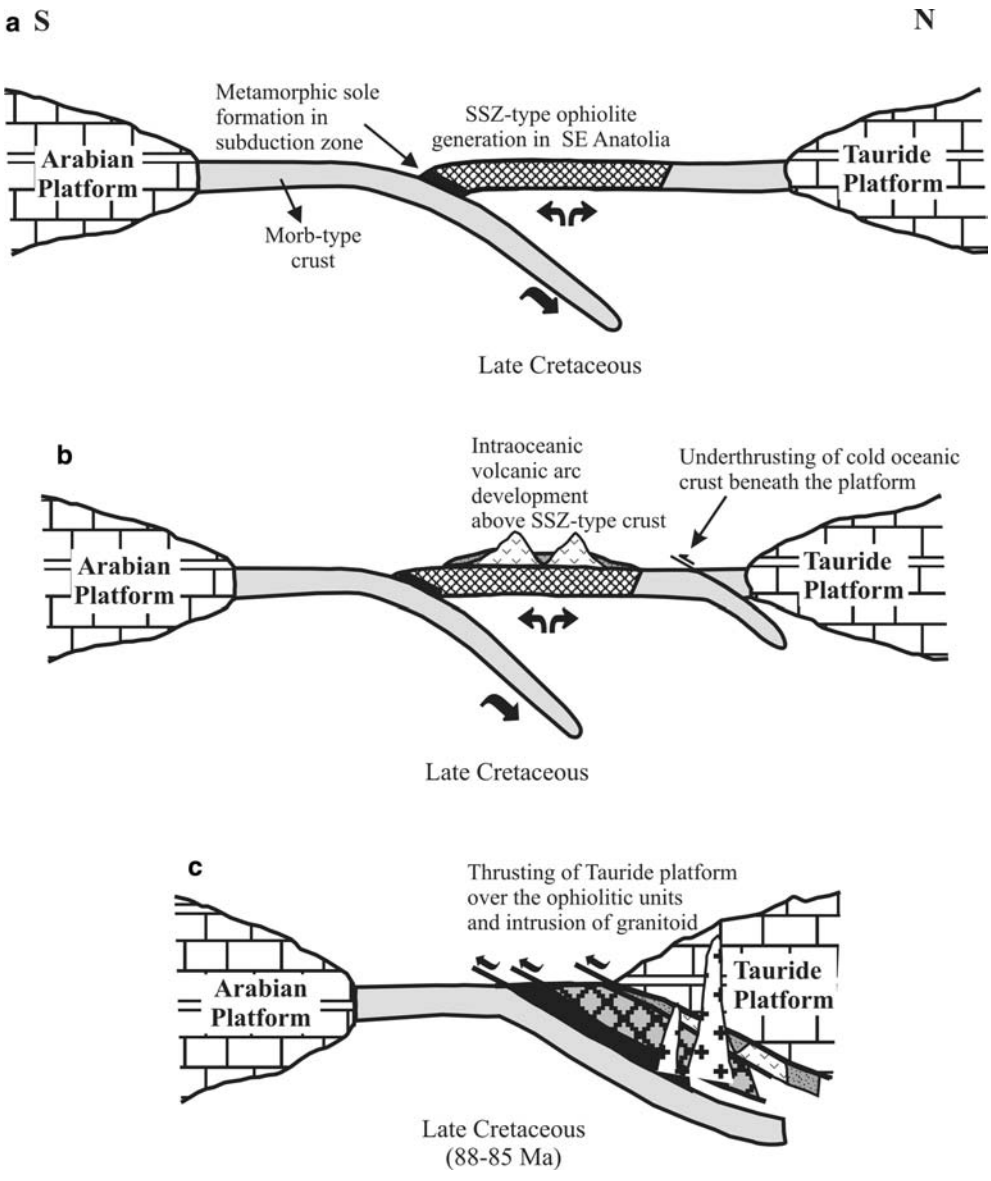

Fig. 13 Tectonic model for the genesis of the ophiolites, related metamorphic units and granitoids in the southeast Anatolia. See text for discussion

Malatya–Keban platform as Coniacian-Santonian (~88–85 Ma).

3. The major, trace and rare earth element geochemistry of the granitoid rocks show that they are typical I-type, calcalkaline volcanic arc granites which formed along the Tauride active continental margin as a result of north-dipping subduction of the southern Neotethys in Late Cretaceous.
4. The biotite chemistry from the granodiorites also confirm the calc-alkaline geochemical affinity with their MgO (11.85–14.38%), Al_2O_3 (13.51–14.69%), FeO (17.17–19.86%) contents and exhibits close similarities to calc-alkaline granitoids that formed in the other parts of the Neotethyan orogenic belt.
5. The hornblende geobarometers from the granodiorites indicate that the early phases of the granitoid body started to crystallize relatively at greater depth (~10 km) and final crystallization occurred at shallower levels (~3 km) during uplift of the granitoid body.

Acknowledgments This research was partly supported by TÜBİTAK (Scientific and Technical Research Council of Turkey, Project Number: YDABÇAG-199Y011) and Division of the Çukurova University Scientific Research Projects (MMF2001.13). Michel Delaloye is thanked for allowing me to use XRF and K–Ar facilities in the Mineralogy Department at Geneva University (Switzerland). Volker Höck is thanked for free access to microprobe facilities in the Geology Department at Salzburg University (Austria). Utku Bağcı and Tamer Rızaoğlu are thanked for their field assistancy. Osman Parlak also acknowledges the financial support from the Turkish Academy of Sciences, in the frame of the Young Scientist Award Program (TÜBA-GEBİP). Nurdane İlbeyli and Yann Rolland are thanked for reviewing the first version of the manuscript. Thanks are due to Prof. Alastair Robertson who reviewed the revised version of the present manuscript.

References

Abdel-Rahman AFM (1994) Nature of biotites from alkaline, calc-alkaline and peraluminous magmas. J Petrol 35:525–541

Aktaş G, Robertson AHF (1984) The Maden complex, SE Turkey: evolution of a Neotethyan continental margin. In: Dixon JE, Robertson AHF (eds) The geological evolution of the eastern Mediterranean. Geological Society of London Special Publication, vol 17, pp 375–402

Aktaş G, Robertson AHF (1990) Tectonic evolution of the Tethys suture zone in S.E. Turkey: evolution evidence from the petrology and geochemistry of Late Cretaceous and Middle Eocene extrusives. In: Malpas J, Moores E, Panayiotou A, Xenophontos C (eds) Ophiolites-oceanic crustal analogues. Proceedings of Troodos ophiolite symposium, Geological Survey, Cyprus 1987, pp 311–329

Arslan M, Kolaylı H, Temizel İ (2004) Güre (Giresun, KD Türkiye) granitoyidinin petrografik, jeokimyasal ve petrolojik özellikleri. Yerbilimleri 30:1–21

Beyarslan M, Bingöl AF (2000) Petrology of a supra-subduction zone ophiolite (Elazığ, Turkey). Can J Earth Sci 37:1411–1424

Boztuğ D, Jonkheere R, Wagner GA, Yeğingil Z (2004) Slow Senonian and fast Paleocene-Early Eocene uplift of the granitoids in the central eastern Pontides, Turkey: apatite fission-track results. Tectonophysics 382:213–228

Brown GC, Thorpe RS, Webb PC (1984) The geochemical characteristics of granitoids in contrasting arcs and comments on magma sources. J Geol Soc Lond 141:413–426

Şengör AMC, Yılmaz Y (1981) Tethyan evolution of Turkey: a plate tectonic approach. Tectonophysics 75:181–241

Cox A, Dalrymple GB (1967) Statistical analysis of geomagnetic reversals data and the precision of potassium–argon dating. J Geophys Res 72:2603–2614

Crawford MB, Searle MP (1992) Field relationships and geochemistry of precollisional (India–Asia) granitoid magmatism in the central Karakoram, northern Pakistan. Tectonophysics 206:171–192

Debon F, Le Fort P, Dautel D, Sonet J, Zimmermann JL (1987) Granites of western Karakoram and northern Kohistan (Pakistan): a composite Mid-Cretaceous to Upper Cenozoic magmatism. Lithos 20:19–40

Dilek Y, Thy P, Hacker B, Grundvig S (1999) Structure and petrology of Tauride ophiolites and mafic dyke intrusions (Turkey): implications for the Neotethyan ocean. Bull Geol Soc Am 111:1192–1216

Faure G (1986) Principles of isotope geology. Wiley, New York, pp 1–589

Fuhrman ML, Lindsley DH (1988) Ternary feldspar modelling and thermometry. Am Mineral 73:201–215

Genç ŞC, Yiğitbaş E, Yılmaz Y (1993) Berit metaofiyolitinin jeolojisi. In: Proceedings of Suat Erk Geol symposium, Ankara University, Geology Department, Turkey, pp 37–52

Hall R (1976) Ophiolite emplacement and the evolution of the Taurus suture zone, south-east Turkey. Bull Geol Soc Am 87:1078–1088

Hammarstrom JM, Zen EA (1986) Aluminum in hornblende: an empirical igneous geobarometer. Am Mineral 71:1297–1313

Harker A (1909) The natural history of igneous rocks. Macmillan, New York

Harris NBW, Pearce JA, Tindle AG (1986) Geochemical characteristics of collision-zone magmatism. In: Coward MP, Ries AC (eds) Collision tectonics. Geological Society of London Special Publication, vol 19, pp 67–81

Hollister LS, Grissom GC, Peters EK, Stowell HH, Sisson VB (1987) Confirmation of the empirical correlation of Al in hornblende with pressure of solidification of calc-alkaline plutons. Am Mineral 72:231–239

Irvine TN, Baragar WRA (1971) A guide to the chemical classification of the common volcanic rocks. Can J Earth Sci 8:523–548

Johnson MC, Rutherford MJ (1989) Experimental calibration of the aluminum in hornblende geobarometer with application to Long Valley caldera (California) volcanic rocks. Geology 17:837–841

Karig DE, Kozlu H (1990) Late Paleogene–Neogene evolution of the triple junction near Maraş, south-central Turkey. J Geol Soc 147:1023–1034

Karslı O, Aydın F, Sadıklar MB (2004) Magma interaction recorded in plagioclase zoning in granitoid systems, Zigana granitoid, Eastern Pontides, Turkey. Turk J Earth Sci 13:287–305

Kelling G, Gökçen SL, Floyd PA, Gökçen N (1987) Neogene tectonics and plate convergence in the eastern Mediterranean: new data from southern Turkey. Geology 15:425–429

Ketin İ (1983) Türkiye Jeolojisine genel bir bakış. İTÜ Kütüphanesi, vol 1259, 595 pp

Le Maitre RW (1989) A classification of igneous rocks and glossary terms. Blackwell, Oxford, pp 1–193

Leake EB, Wooley AR, Arps CES, Birch WD, Gilbert MC, Grice JD, Hawthorne FC, Kato A, Kisch HJ, Krivovichev VG, Linthout K, Laird J, Mandarino J, Maresch WV, Nickhel EH, Rock NMS, Schumacher JC, Smith DC, Stephenson NCN, Ungaretti L, Whittaker EJW, Youzhi G (1997) Nomenclature of amphiboles. Eur J Min 9:623–651

Maniar PD, Piccolli PM (1989) Tectonic discrimination of granitoids. Bull Geol Soc Am 101:636–643

Michard A, Whitechurch H, Ricou LE, Montigny R, Yazgan E (1984) Tauric subduction (Malatya-Elazığ provinces) and its bearing on tectonics of the Tethyan realm in Turkey. In: Dixon JE, Robertson AHF (eds) The geological evolution of the eastern Mediterranean. Geological Society of London Special Publication, vol 17, pp 361–374

MTA (2002) 1/500.000 scale geological maps of Turkey. General Directorate of Mineral Research and Exploration, Ankara, Turkey

Mukasa SB, Ludden JN (1987) Uranium–lead ages of plagiogranites from the Troodos ophiolite. Cyprus, and their tectonic significance. Geology 1:825–828

Parlak O, Rızaoğlu T (2004) Geodynamic significance of granitoid intrusions in the southeast Anatolian orogeny (Turkey). In: Proceedings of the 5th international eastern Mediterranean geological symposium, Thessaloniki Greece, 14–20 April 2004, Abstr 157

Parlak O, Önal A, Höck V, Kürüm S, Delaloye M, Bağcı U, Rızaoğlu T (2002) Inverted metamorphic zonation beneath the Yüksekova ophiolite in SE Anatolia. In: Proceedings of the 1st international symposium of the Faculty of Mines (ITU) on Earth sciences and engineering, 16–18 May, Istanbul, Turkey, p 133

Parlak O, Höck V, Kozlu H, Delaloye M (2004) Oceanic crust generation in an island arc tectonic setting, SE Anatolian orogenic belt (Turkey). Geol Mag 141:583–603

Pearce JA, Harris NBW, Tindle AG (1984) Trace element discrimination diagrams for the tectonic interpretation of granitic rocks. J Petrol 25:956–983

Perinçek D, Kozlu H (1984) Stratigraphy and structural relations of the units in the Afşin–Elbistan–Doğanşehir region (Eastern Taurus). In: Proceedings of the international symposium, Geology of Taurus Belt, MTA, Ankara-Turkey, pp 181–198

Petterson MG, Windley BF (1985) Rb–Sr dating of the Kohistan arc-Batholith in the trans Himalayan of N. Pakistan and tectonic implications. Earth Planet Sci Lett 74:45–75

Pickett EA, Robertson AHF (1996) Formation of the Late Palaeozoic to Early Mesozoic Karakaya complex and related ophiolites in NW Turkey by palaeotethyan subduction-accretion. J Geol Soc Lond 153:995–1009

Rızaoğlu T, Parlak O, İşler F (2004) Geochemistry and tectonic setting of the Kömürhan ophiolite in southeast Anatolia. In: Proceedings of the 5th international eastern Mediterranean geology symposium, Thessaloniki, Greece, 14–20 April 2004, Abstract 285

Robertson AHF (1998) Mesozoic-Tertiary tectonic evolution of the easternmost Mediterranean area; integration of marine and land evidence. In: Robertson AHF, Emeis KC, Richter KC, Camerlenghi A (eds) Proceedings of the Ocean Drilling Program, science results, vol 160, pp 723–782

Robertson AHF (2000) Mesozoic-Tertiary tectonic-sedimentary evolution of a south Tethyan oceanic basin and its margins in southern Turkey. In: Bozkurt E, Winchester JA, Piper JDA (eds) Tectonics and magmatism in Turkey and the surrounding area. Geological Society of London Special Publication, vol 173, pp 97–138

Robertson AHF (2002) Overview of the genesis and emplacement of Mesozoic ophiolites in the Eastern Mediterranean Tethyan region. Lithos 65:1–67

Robertson AHF, Dixon JE (1984) Introduction: aspects of the geological evolution of the Eastern Mediterranean. In: Dixon JE, Robertson AHF (eds) The geological evolution of the eastern Mediterranean. Geological Society of London Special Publication, vol 17, pp 1–74

Robertson AHF, Ünlügenç UC, İnan N, Taslı K (2004) The Misis–Andırın complex: a Mid-Tertiary melange related to late-stage subduction of the Southern Neotethys in S Turkey. J Asian Earth Sci 22:413–453

Robertson AHF, Ustaömer T, Parlak O, Ünlügenç UC, Taslı K, İnan N (2006a) Late Cretaceous–Early Tertiary tectonic evolution of south-Neotethys in SE Turkey: evidence from the Tauride thrust belt in SE Turkey (Binboğa-Engizek segment). J Asian Earth Sci (in press)

Robertson AHF, Parlak O, Rızaoğlu T, Ünlügenç UC, İnan N, Taslı K, Ustaömer T (2006b) Late Cretaceous-Mid Tertiary tectonic evolution of the eastern Taurus Maountains and the Southern Tethyan ocean evidence from the Elazığ region, SE Turkey. Geological Society of London Special Publication (in press)

Rolland Y, Picard C, Pecher A, Lapierre H, Bosch D, Keller F (2002) The Cretaceous Ladakh arc of NW himalayan-slab melting and melt-mantle interaction during fast northward drift of Indian plate. Chem Geol 182:139–178

Rollinson H (1993) Using geochemical data: evaluation, presentation, interpretation. Longman Group, UK, pp 1–352

Schmidt MW (1992) Amphibole composition in tonalite as a function of pressure: an experimental calibration of the Al in hornblende barometer. Contrib Mineral Petrol 110:304–310

Spear JA (1981) An experimental study of hornblende stability and compositional variability in amphibolite. Am J Sci 281:697–734

Speer JA (1984) Micas in igneous rocks. Rev Mineral 13:299–356

Steiger RH, Jager E (1977) Subcommission on geochronology: convention on the use of decay constants in geo- and cosmochronology. Earth Planet Sci Lett 36:359–362

Sun SS, McDonough WF (1989) Chemical and isotopic systematics of oceanic basalts: implications for mantle composition and processes. In: Saunders AD, Norry MJ (eds) Magmatism in the ocean basins. Geological Society of London Special Publication, vol 42, pp 313–347

Tarhan N (1986) Doğu Toroslarda Neotetisin kapanımına ilişkin granitoyid magmalarının evrimi ve kökeni. MTA Dergisi 107:95–112

Wilson M (1989) Igneous petrogenesis: a global tectonic approach. Chapman and Hall, London, pp 1–466

Yazgan E, Chessex R (1991) Geology and tectonic evolution of the southeastern Taurides in the region of Malatya. Turk Assoc Petrol Geol 3:1–42

Yılmaz Y (1990) Allochthonous terranes in the Tethyan middle east: Anatolia and surrounding regions. R Soc Lond Philos Trans A 331:611–624

Yılmaz Y (1993) New evidence and model on the evolution of the southeast Anatolian Orogen. Bull Geol Soc Am 105:251–271

Yılmaz Y, Gürpınar O, Kozlu H, Gül MA, Yiğitbaş E, Yıldırım M, Genç ŞC, Keskin M (1987) Kahramanmaraş Kuzeyinin Jeolojisi (Andırın-Berit-Engizek-Nurhak-Binboğa Dağları), Türkiye Petrolleri A.O. Rapor No: 2028, Ankara, p 218

Yılmaz Y, Yiğitbaş E, Genç ŞC (1993) Ophiolitic and metamorphic assemblages of southeast Anatolia and their significance in the geological evolution of the orogenic belt. Tectonics 12:1280–1297